New age constraints support a K/Pg boundary interval on Vega Island, Antarctica: Implications for latest Cretaceous vertebrates and paleoenvironments

Eric M. Roberts[1,†], Patrick M. O'Connor[3,4], Julia A. Clarke[5], Sarah P. Slotznick[6], Christa J. Placzek[2], Thomas S. Tobin[7], Carey Hannaford[8], Theresa Orr[1], Zubair A. Jinnah[9], Kerin M. Claeson[10], Steven Salisbury[11], Joseph L. Kirschvink[12], Duncan Pirrie[13], and Matthew C. Lamanna[14]

[1]*Earth and Environmental Sciences, James Cook University, Townsville, Queensland 4811, Australia*
[2]*Australian Groundwater & Environmental Consultants Pty Ltd., 1/60 Ingham Road, West End, Queensland 4810, Australia*
[3]*Department of Biomedical Sciences, Heritage College of Osteopathic Medicine, Ohio University, Athens, Ohio 45701, USA*
[4]*Ohio Center for Ecological and Evolutionary Studies, Ohio University, Athens, Ohio 45701, USA*
[5]*Department of Geological Sciences, University of Texas at Austin, 1 University Station, C1100, Austin, Texas 78712, USA*
[6]*Department of Earth Sciences, Dartmouth College, Hanover, New Hampshire 03755, USA*
[7]*Department of Geological Sciences, University of Alabama, Tuscaloosa, Alabama 35401, USA*
[8]*MGPalaeo, Malaga WA 6090, Australia*
[9]*School of Geosciences, University of the Witwatersrand, Johannesburg, South Africa*
[10]*Department of Biomedical Sciences, Philadelphia College of Osteopathic Medicine, Philadelphia, Pennsylvania 19131, USA*
[11]*School of Biological Sciences, The University of Queensland, Brisbane, Queensland 4072, Australia*
[12]*Division of Geological and Planetary Sciences, California Institute of Technology, Pasadena, California 91125, USA*
[13]*School of Applied Science, University of South Wales, Pontypridd C37 4BD, UK*
[14]*Section of Vertebrate Paleontology, Carnegie Museum of Natural History, 4400 Forbes Avenue, Pittsburgh, Pennsylvania 15213, USA*

ABSTRACT

A second K/Pg boundary interval in the northern sector of the Antarctic Peninsula on Vega Island has been proposed, yet current temporal resolution of these strata prohibits direct testing of this hypothesis. To not only test for the existence of a K/Pg boundary on Vega Island but also provide increased age resolution for the associated vertebrate fauna (e.g., marine reptiles, non-avian dinosaurs, and avian dinosaurs), the Vega Island succession was intensively re-sampled. Stratigraphic investigation of the Cape Lamb Member of the Snow Hill Island Formation, and in particular, the overlying Sandwich Bluff Member of the López de Bertodano Formation, was conducted using biostratigraphy, strontium isotope stratigraphy, magnetostratigraphy, and detrital zircon geochronology. These data indicate a Late Campanian–early Maastrichtian age for the Cape Lamb Member and pres-ent three possible correlations to the global polarity time scale (GPTS) for the overlying Sandwich Bluff Member. The most plausible correlation, which is consistent with biostratigraphy, detrital zircon geochronology, sequence stratigraphy, and all but one of the Sr-isotope ages, correlates the base of the section to C31N and the top of the section with C29N, which indicates that the K/Pg boundary passes through the top of the unit. A second, less plausible option conflicts with the biostratigraphy and depends on a series of poorly defined magnetic reversals in the upper part of the stratigraphy that also correlates the section between C31N and C29R and again indicates an inclusive K/Pg boundary interval. The least likely correlation, which depends on favoring only a single Sr-isotope age at the top of the section over biostratigraphy, correlates the section between C31N and C30N and is inconsistent with an included K/Pg boundary interval. Although our preferred correlation is well supported, we failed to identify an Ir-anomaly, spherules/impact ejecta, or other direct evidence typically used to define the precise position of a K/Pg boundary on Vega Island. This study does, however, confirm that *Vegavis*, from the base of the Sandwich Bluff Member, is the oldest (69.2–68.4 Ma) phylogenetically placed representative of the avian crown clade, and that marine vertebrates and non-avian dinosaurs persisted in Antarctica up to the terminal Cretaceous.

INTRODUCTION

Upper Cretaceous sedimentary rocks exposed in the Antarctic Peninsula region preserve one of the most important and continuous high-latitude records of faunal evolution and paleoclimatic change leading up to and through the Cretaceous/Paleogene (K/Pg) extinction event. These strata, deposited within the James Ross Basin, preserve an extensive record of marine invertebrate and vertebrate fossils, along with rare continental vertebrates, including birds and non-avian dinosaurs (e.g., Chatterjee, 2002; Case et al., 2000; Clarke et al., 2005, 2016; Reguero and Gasparini, 2006; Tambussi and Acosta Hospitaleche, 2007; Cerda et al., 2012; Coria et al., 2013; Reguero et al., 2013a, 2013b; Rozadilla et al., 2016; Acosta Hospitaleche et al., 2019; Ely and Case, 2019; Lamanna et al.,

Eric M. Roberts [ORCID] https://orcid.org/0000-0002-8583-7437
†eric.roberts@jcu.edu.au.

https://doi.org/10.1130/B36422.1; 8 figures; 2 tables; 1 supplemental file.

2019; Tambussi et al., 2019; Cordes-Person et al., 2020). Significant stratigraphic and paleontological efforts (e.g., Macellari, 1988; Elliot et al., 1994; Tobin et al., 2012) in the basin have focused on the well-documented K/Pg boundary section on Seymour Island in the southeastern and more distal part of the basin. A wealth of recent work has also focused on the Cretaceous units on James Ross Island, leading to the discovery of important vertebrate fossil localities. Work to constrain both the age and depositional setting of these localities has also improved basin stratigraphy, particularly for the Coniacian to lower Campanian Hidden Lake, Santa Marta, and lower Snow Hill Island Formations (Milanese et al., 2017, 2019, 2020).

The northwestern part of the basin includes Humps Island and Vega Island, both of which also expose Upper Cretaceous strata (del Valle and Medina, 1980; Pirrie et al., 1991; Olivero et al., 1992; Pirrie, 1994; Marenssi et al., 2001; Smith, 1992). Although the fossil record from Humps Island is quite limited, Vega Island has produced important continental vertebrate fossils, and it is possible that the K/Pg boundary occurs at the top of the exposed section (Roberts et al., 2014). Unfortunately, strata across the basin have proven difficult to precisely correlate, particularly among the various islands due to both cover and accessibility. Additionally, correlation with better dated K/Pg sections in the Northern Hemisphere has also been challenging (e.g., Crame et al., 1999; McArthur et al., 2000). Invertebrate biostratigraphy has been utilized to establish a basic stratigraphic framework across the basin (e.g., Olivero, 2012), but issues related to the interpretation of localized extinction and endemism have proven problematic, particularly for any extra-basinal correlative inferences (Macellari, 1988; Olivero and Medina, 2000; Milanese et al., 2017).

Recent efforts utilizing magnetostratigraphy have been more successful at resolving stratigraphic uncertainties in selected parts of the basin (Tobin et al., 2012, 2020; Milanese et al., 2017, 2019, 2020), but to date, attempts at radiometric dating and strontium isotope stratigraphy have been limited. Crame et al. (1999, 2004) and McArthur et al. (1998, 2000) first utilized strontium isotope stratigraphy to establish a number of key control points in the basin, including an important temporal calibration within the *Gunnarites antarcticus* faunal assemblage in the Cape Lamb Member of the Snow Hill Island Formation on Vega Island (Ammonite Assemblage 10 of Olivero, 2012). Although devitrified volcanic ash beds (bentonites) have been reported throughout the stratigraphy (e.g., Bowman et al., 2016), few published radiometric ages exist. However, Tobin et al. (2020) recently

highlighted the potential for utilizing detrital zircon geochronology to establish better age control for poorly dated Upper Cretaceous strata on Robertson Island in the southern James Ross Basin through the identification of the youngest populations of syndepositionally derived volcanic grains in the abundant volcanolithic sandstone units within the basin.

Reconstructions of the regional Upper Cretaceous stratigraphy, paleoenvironments, and paleogeography of the James Ross Basin are complicated by the long distances between the islands and the variability in thickness and quality of exposures, which ranges from exquisite to poor. The best-characterized and most continuous exposures are recorded on Seymour Island and the regularly exposed portion of Snow Hill Island in the southern, distal portion of the basin. In contrast, deposits in the northern, proximal part of the basin (e.g., particularly those on Vega Island) are patchier in nature and complicated by faulting, intrusive sills and dykes, and overlying volcanics, which renders them generally less well-constrained from a temporal viewpoint. This is problematic because the Upper Cretaceous section on Vega Island preserves a unique lithostratigraphic unit known as the Sandwich Bluff Member (SBM) of the López de Bertodano Formation, a nearshore marine to potentially non-marine (near the top) succession that preserves the richest continental fossil vertebrate assemblage from the Antarctic Peninsula region (Lamanna et al., 2019). This unit is best known for its important avian fossils, including some that are hypothesized to be the geologically earliest representatives (e.g., *Vegavis iaai*; Clarke et al., 2005, 2016) of the avian crown clade. However, poor age control at the top of the Vega Island succession limits our understanding of these and other vertebrate fossils, including the only indisputable hadrosaur from Antarctica (Case et al., 2000) and a suite of other non-avian and avian dinosaur remains (reviewed in Tambussi and Acosta Hospitaleche, 2007; Reguero et al., 2013a; Ksepka and Clarke, 2015; Acosta Hospitaleche et al., 2019; Lamanna et al., 2019).

This study integrates Sr-isotope stratigraphy, palynology, macrofossil biostratigraphy, magnetostratigraphy, and U-Pb detrital zircon geochronology to refine the age(s) of Upper Cretaceous strata on Vega Island. The aims are threefold and include: (1) establishing a robust chronostratigraphy for the stratigraphic succession on Vega Island; (2) testing the hypothesis that a K/Pg boundary interval is preserved at the top of the Sandwich Bluff Member of the López de Bertodano Formation; and (3) refining the age of strata that yield the marine vertebrate, non-avian dinosaur, and bird fossils, including *Vegavis iaai*,

a taxon that represents one of the oldest-known records of the avian crown group.

GEOLOGIC BACKGROUND

Strata in the James Ross Basin comprise only the exposed portion of the much larger Larsen Basin (Macdonald et al., 1988), which developed in a back-arc basin framework behind the Graham Land magmatic arc during the Cretaceous and Paleogene (Fig. 1A). The Graham Land arc developed on what is now the Antarctic Peninsula due to southeast-directed subduction of the proto-Pacific Plate (Hathway, 2000). Nearly 7000 m of Cretaceous–Paleogene clastic strata were deposited in the James Ross Basin and represent three major depositional cycles: the Aptian–Coniacian Gustav Group, the overlying Santonian–Danian Marambio Group, and the Selandian–Priabonian? Seymour Island Group (Rinaldi et al., 1978; Olivero et al., 1986; Pirrie, 1989; Crame et al., 1991; Pirrie et al., 1991; Olivero, 2012; Crame, 2019). The succession reveals deeper water facies in the Gustav Group, followed by shallowing up of the Marambio Group that is associated with some combination of basin filling, uplift, and sea-level change during the terminal Cretaceous and early–mid Paleogene (Hathway, 2000). Deposition took place across a broad shelf that extended >100 km from shore to slope (Pirrie et al., 1991; Hathway, 2000). Sea-level fluctuations had a significant influence on the depositional patterns and geometry of the succession, and these are generally linked to third-order eustatic sea-level cycles that can be traced across the basin (Olivero, 2012).

Over the last 100 + years, Cretaceous and Paleogene strata of the James Ross Basin have been subject to considerable attention from paleontologists interested in high-latitude paleoenvironments, paleoclimate, and evolutionary patterns (e.g., Wilckens, 1911; Zinsmeister, 1979, 1982, 2001; Olivero et al., 1986, 1992, 2008; Askin, 1988; Zinsmeister et al., 1989; Crame et al., 1991, 2004; Pirrie et al., 1991; Marenssi et al., 1992, 2001; Riding et al., 1992; Wood and Askin, 1992; Bowman et al., 2012, 2013, 2016; Olivero, 2012; di Pasquo and Martin, 2013; Witts et al., 2015, 2016, 2018; Petersen et al., 2016; Schoepfer et al., 2017; Tobin, 2017, Hall et al., 2018; Crame, 2019; Whittle et al., 2019; Mohr et al., 2020). To date, much of this work has been focused on the Marambio Group, involving paleontological exploration coupled with detailed sedimentological investigations of the deposits that are exposed principally on Seymour, Snow Hill, James Ross, Humps, Cockburn, and Vega Islands. Exposures range from exceptional and extensive, as on Seymour and
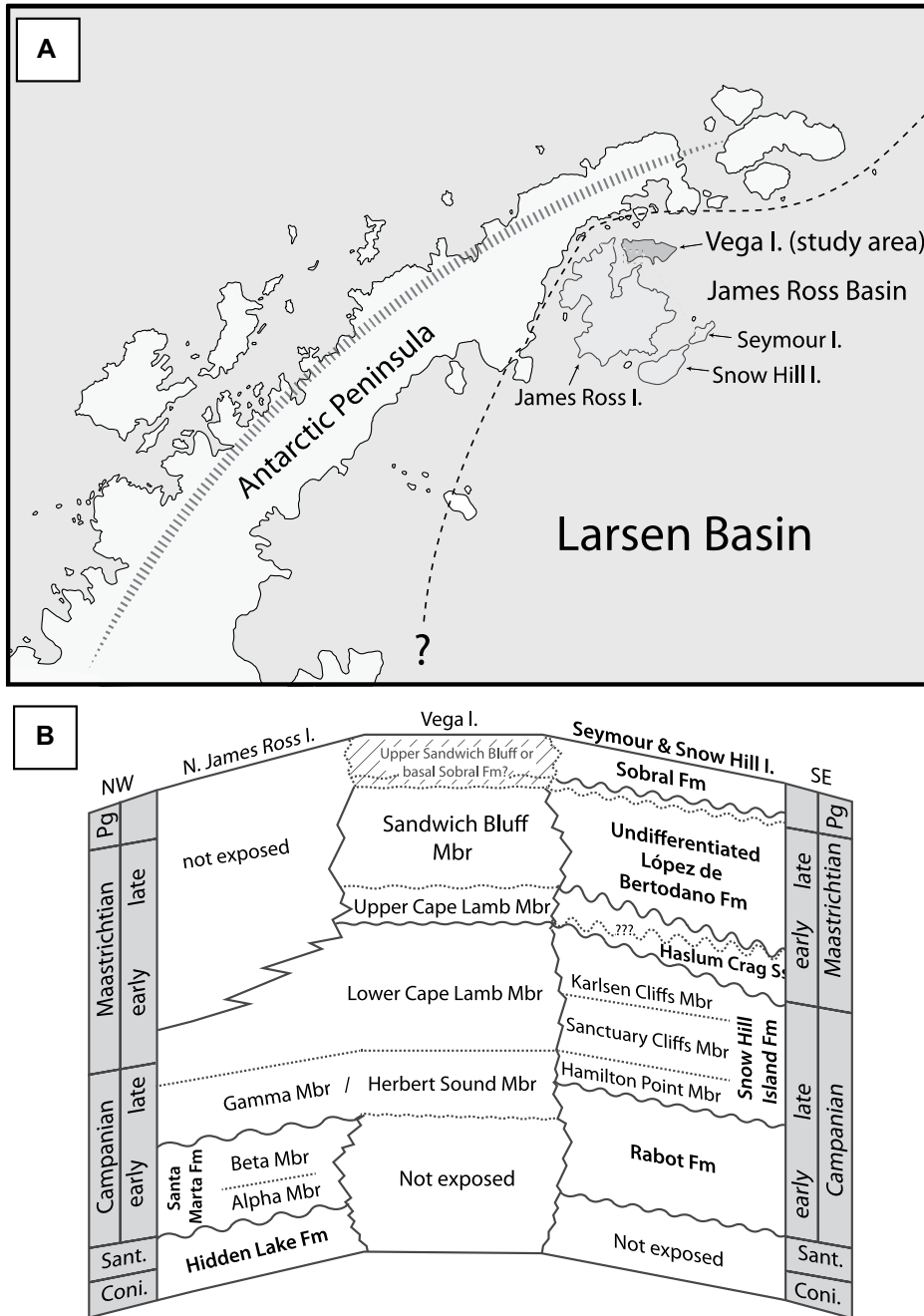
Figure 1. Location and stratigraphy of main study area are shown (modified after Crame et al., 2004; Roberts et al., 2014; Tobin et al., 2020, and references therein). (A) Map of northern Antarctic Peninsula (white) indicates islands (light gray) with Upper Cretaceous exposures in the James Ross Basin. Note that the main study location, Vega Island, is dark gray. Dotted line through islands indicates cross-section trace for correlation chart in panel B; thick dashed line indicates hypothesized margins of Larsen Basin (which includes James Ross Basin) (modified from del Valle et al., 1992); arcuate dashed line through peninsula represents highly generalized location of Graham Land magmatic arc. (B) Simplified correlation chart of Upper Cretaceous to basal Paleogene stratigraphic units within the James Ross Basin. Formation (Fm) and member (Mbr) names follow Olivero (2012), though the Alpha and Beta Members of the Santa Marta Formation are roughly equivalent to the Lachman Crags Member of Pirrie et al. (1997), and the Gamma Member of the Snow Hill Island Formation is roughly equivalent to the Herbert Sound Member of Crame et al. (1991). I—island; Pg—Paleogene; Ss—Sandstone.

northern Snow Hill Islands, to isolated and variably covered by ice and younger volcanic rocks, as on James Ross and Vega Islands.

Vega Island

Cretaceous outcrops on Vega Island are concentrated on Cape Lamb (Fig. 1B). Here, a partial section of the Campanian Gamma Member (Herbert Sound Member) of the Snow Hill Island Formation (~50 m thick) forms the base of the section and is overlain by the Upper Campanian to lower Maastrichtian Cape Lamb Member of the Snow Hill Island Formation (~330 m thick). These are, in turn, capped by the ~100–110-m-thick Maastrichtian Sandwich Bluff Member of the López de Bertodano Formation (Pirrie et al., 1991; Olivero et al., 1992; Marenssi et al., 2001; Roberts et al., 2014). The Sandwich Bluff Member is widely recognized for its unique sample of high-latitude latest Cretaceous terrestrial vertebrate fossils from the Southern Hemisphere (e.g., Case et al., 2000; Clarke et al., 2005, 2016; Tambussi and Acosta Hospitaleche, 2007; Cerda et al., 2012; Coria et al., 2013; Reguero et al., 2013a, 2013b; Rozadilla et al., 2016; Acosta Hospitaleche et al., 2019; Lamanna et al., 2019). In particular, the holotype and referred partial skeletons of *Vegavis* (Clarke et al., 2005, 2016) and other significant bird specimens (Acosta Hospitaleche et al., 2019; West et al., 2019), as well as rare, non-avian dinosaur material have been discovered from the Sandwich Bluff Member (Lamanna et al., 2019). The holotype and referred skeletons of *Vegavis* and other, as-yet undescribed avian fossils, were collected from the basal unit of the Sandwich Bluff Member (Clarke et al., 2005, 2016; SBM1 of Roberts et al., 2014). Most estimates of the age of the Sandwich Bluff Member on Vega Island are based on biostratigraphic data and long-distance correlations with better-studied exposures of the López de Bertodano Formation on Seymour Island (Pirrie et al., 1991; Bowman et al., 2012, 2014).

Biostratigraphic refinement and taxonomic revision of Antarctic records of the dinoflagellate cyst *Manumiella* led to description of the new species *M. bertodano* (Thorn et al., 2009; Bowman et al., 2012, 2014), which was originally identified as "*Manumiella* n.sp. 2" by Pirrie et al. (1991) from the Sandwich Bluff Member of Vega Island. On Seymour Island, this species is restricted to near the top of the Upper Maastrichtian López de Bertodano Formation (upper unit 9; ca. 67.7–66.3 Ma) with a range terminating below the boundary (Bowman et al., 2012, 2014). Although most previous workers conclude that the section exposed on Vega Island terminated prior to the K/Pg boundary, Roberts

et al. (2014) identified a rapid, proximal shoreline shift recorded by an erosional, channel-filled alluvial conglomerate 20 m below the top of the section. This was succeeded by rapid facies deepening and a return to marine conditions in the top 10 m of the section. These features were interpreted as evidence of a previously unrecognized sequence boundary in the northern portion of the basin and compare favorably with a notable sequence boundary between the top of the López de Bertodano and Paleogene-age Sobral Formations on Seymour Island. The conceptual early Paleocene sequence boundary on Seymour Island caps the *Maorites* and *Grossouvrites* (MG) sequence of Olivero (2012; but also see Olivero and Medina, 2000).

Previous biostratigraphic work on Vega Island by Pirrie et al. (1991) and Riding (1997, unpublished report) regarded the occurrence of *M. bertodano* (their "*M.* n. species 2") as extending from near the base of the Sandwich Bluff Member to ~8.4 m below the top unit. Thorn et al. (2009) and Bowman et al. (2012, 2014) considered the upper limit of *M. bertodano* on Seymour Island to terminate ~50–100 m below the K/Pg boundary in their composite section. However, the Sandwich Bluff Member on Vega Island is proximal to the Cretaceous shoreline and considerably condensed relative to the López de Bertodano Formation on Seymour Island (Olivero, 2012). Roberts et al. (2014) suggested the possibility that a thin interval of Paleogene strata may be exposed on Vega Island. These workers had no biostratigraphic, geochronologic, or geochemical evidence to support the hypothesized K/Pg boundary on this island. However, recognition of a possible sequence boundary near the top of the Sandwich Bluff Member was suggested to correlate to a post-Cretaceous sea-level fall elsewhere in the basin. Hence, this presents tantalizing evidence suggesting that this important event in Earth history may be recorded on Vega Island, or perhaps that the tectonic/eustatic history of the James Ross Basin is more complex than previously considered, with an undocumented sea-level fall occurring just prior to the K/Pg boundary in the northern part of the basin.

METHODS

The research presented herein was based on field observations and sampling conducted during two cruises to the James Ross Basin sponsored by the U.S. National Science Foundation aboard the U.S. Antarctic Program (USAP) vessels *R/V Lawrence M. Gould* and *R/V Nathaniel B. Palmer* during the austral summers of 2011 and 2016, respectively. Fieldwork was carried out primarily from base camps on Vega Island, with the addition of USAP-mediated helicopter

support in 2016. Data used in different analyses (e.g., detrital zircon and Sr-isotope geochronology, etc.) were collected from strata exposed on Vega Island; specific stratigraphic intervals for a given analysis are detailed in the sections below.

Sedimentology

Over three days during the 2016 field season, a detailed stratigraphic section was re-measured through the upper portion of the Sandwich Bluff section. This section began at the base of unit SBM14 and extended through the interval that Roberts et al. (2014) hypothesized could be correlative with the Sobral Formation (SF1 and SF2) on Seymour Island. To minimize confusion, strata above SBM15 are collectively referred to in the present study as SBM16 (instead of SF1 and SF2 as in Roberts et al., 2014), but they have been broken down into 10 discrete subunits within that interval (SBM16a–SBM16j). A Jacob's staff and Brunton compass were used to measure this interval at the decimeter scale. Particular attention was paid to searching for evidence of the K/Pg boundary interval through this section, including evidence of a fish kill horizon or glauconite layer as observed on Seymour Island (Elliot et al., 1994; Zinsmeister, 1998). Sediment sampling for geochemistry, detrital zircon geochronology, and palynology was conducted, with detailed descriptions of the sedimentology, ichnology, and paleontology recorded (Fig. 2).

Sr-Isotope Analysis

A total of 26 aragonitic ammonite, nautiloid, and bivalve shells, along with two calcitic pycnodont oyster shells, were selected and sampled for in situ Sr-isotope analysis. All were identified and collected during 2016, and the shells were selected from a large collection of fossils sampled throughout the stratigraphic succession on Vega Island. Only shells in the best condition were initially selected, with the least visually altered portions of these shells imaged using scanning electron microscopy (SEM) and evaluated for preservation and diagenesis based on the methods described by Cochran et al. (2010) and Knoll et al. (2016) (see Supplemental Material[1]). Due to the typically small amount of well-preserved shell (or regions of shell) associated with the samples, repeat analyses could only be performed on nine of the 28,

[1]Supplemental Material. Figures S1–S7 and Tables S1 and S2. Please visit https://doi.org/10.1130/GSAB.S.19878295 to access the supplemental material, and contact editing@geosociety.org with any questions.

which resulted in 37 total Sr-isotope analyses by coauthor Christa Placzek (Table 1). Detailed sampling, taphonomic filtering, sample preparation, and analytical methods are further outlined in the Supplemental Material.

Due to the thickness of the section and the patchy nature of well-preserved fossils in the Cape Lamb and Sandwich Bluff members, this study focused on fossil collections from seven different stratigraphic intervals (see Table 1; Fig. 3 for details). Analyses of the fossils within each of these major stratigraphic intervals were binned together to obtain a mean $^{87}Sr/^{86}Sr$ ratio. Note that both benthic and nekto-benthic forms and calcitic and aragonitic shells were binned together due to the limited number of samples available. These values were used to determine a numerical age for the eight intervals and the uncertainty limits on each age using the newest version (V5, provided by J. McArthur, 2014 and 2017, personal commun.) of the Locally Weighted Scatterplot Smoothing (LOWESS) look-up table (Howarth and McArthur, 1997). Following Crame et al. (1999), the uncertainty of each age includes the uncertainty inherent in the reference curve of McArthur and Howarth (1998) using updated Version 5 paired with the GTS2012 in McArthur et al. (2012) (Table 1; Fig. 3). This approach follows that used by Crame et al. (1999) in their seminal work on the Sr-isotope stratigraphy of the Upper Cretaceous succession in the James Ross Basin. We also recalibrated the robust $^{87}Sr/^{86}Sr$ age published by Crame et al. (1999) for the lower Cape Lamb Member using the updated (v.5) LOWESS curve (Fig. 3).

U-Pb Detrital Zircon Geochronology

Two detrital zircon samples were collected from the Sandwich Bluff Member of the López de Bertodano Formation on Vega Island and analyzed using U-Pb laser ablation–inductively coupled plasma–mass spectrometry (LA-ICP-MS). The lower sample (3-5-11-1) is from a calcareous sandstone concretion collected from the *Vegavis*-bearing unit SBM1 at the base of the Sandwich Bluff Member (see Roberts et al., 2014). The other sample (2-25-16-9) was collected from the top of the Sandwich Bluff Member (SBM16j) from muddy sandstone beds 2.75 m below the unconformably overlying Pliocene Hobbs Glacier Formation. Only one of these two samples (2-25-19-9 from SBM16) yielded a population (n = 3+) of potential syndepositional zircons. Details about mineral separation and the U-Pb LA-ICP-MS methods following those of Todd et al. (2019) and Foley et al. (2021) are provided in the Supplemental Material.

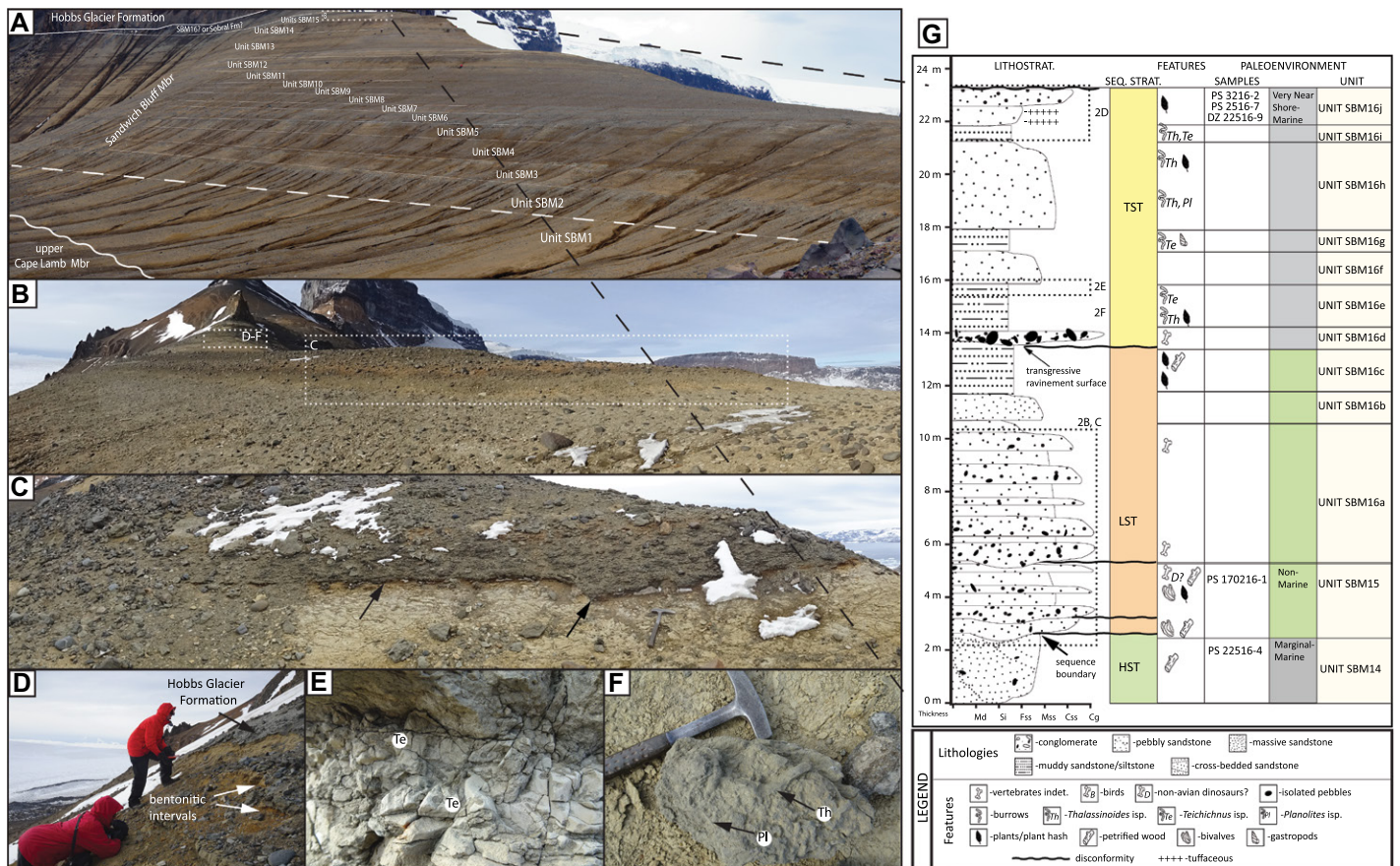The results were processed using the Iolite software package (https://iolite-software.com/),

Figure 2. Detailed sedimentology and stratigraphy of the uppermost Sandwich Bluff Member of the López de Bertodano Formation on Vega Island are shown. (A) Photomosaic shows key stratigraphic units through Sandwich Bluff Member (modified from Roberts et al., 2014). Dashed white box shows location of panel B. (B) View of contacts between unit SBM14/15 and SBM16 (Sobral Formation-equivalent unit?). Dashed white boxes show locations of photos C and D–F. (C) Erosional contact between SBM14/15 and SBM16?/Sobral Formation equivalent? at top of Sandwich Bluff. Black arrows indicate contact. (D) Photo of bentonitic siltstone units at base of unit SBM16j. (E) Intensely bioturbated siltstone (unit SBM16e) with coarse sand infilling from overlying unit (SBM16f). Te—*Teichichnus*, which indicates a return to marine conditions. (F) *Thalassinoides* (Th) and *Planolites* (Pl) burrows at the base of unit SBM16e, which also supports a return to marine conditions. (G) Measured section with sequence stratigraphic interpretations, unit nomenclature, and sample location throughout the upper portion of the Sandwich Bluff Member on Vega Island. Dashed boxes labeled 2B–F next to section show location of those images in the measured section. DZ—detrital zircon sample; HST—highstand systems tract; LST—lowstand systems tract; PS—pollen sample; TST—transgressive systems tract. See inset legend for lithologies and sedimentologic features and both trace and actual fossils.

which corrected for downhole fractionation, instrumental drift, and propagated error estimation (Paton et al., 2011). Probability density plots and weighted mean ages were calculated using Isoplot for the SBM16 sample (Ludwig, 2008). The focus of the detrital zircon analysis in this study was on the youngest zircon populations in the samples so that maximum depositional ages (MDAs) could be calculated to help refine the age of the Sandwich Bluff Member and test the K/Pg boundary hypothesis (Fig. 4). Individual zircon grain ages younger than 300 Ma with >10% discordance between the ^{206}Pb/^{238}U age and the ^{207}Pb/^{235}U age were not included in the study. MDAs were calculated by determining the weighted mean of the youngest cluster of con-

cordant grains (where n ≥ 3) with overlapping ages (within 2σ error) for each sample (Dickinson and Gehrels, 2009; Tucker et al., 2013, 2016). In the lower sample, a population was not identified, so the youngest single grain age is discussed. All syndepositional zircons (younger than 70 Ma) are considered to be derived from nearby volcanic sources; however, a more detailed sedimentary provenance analysis of the detrital zircon populations is beyond the scope of the current investigation.

Macrofossil Biostratigraphy

Marine macrofossils are less common in the Sandwich Bluff Member than in many

other exposures of the James Ross Basin, but we recovered several ammonites that could be placed within our section both as geochemical targets and biostratigraphic markers. When recognizable or well-preserved specimens were observed in the field, they were either collected or photographed in situ. Stratigraphic locality information and GPS locations were recorded. In the lab, specimens were photographed, and taxonomic diagnoses were established by coauthor Thomas Tobin.

Palynology

Four palynology samples from the top of the Sandwich Bluff Member were collected and

TABLE 1. ISOTOPIC AND ELEMENTAL DATA FOR VEGA ISLAND SHELL SAMPLES

Specimen	Sample ID	$^{87}Sr/^{86}Sr$	Error (2σ)	Age	Error	SEM PI	Ba/Ca (mmol/mol)	Fe/Ca (mmol/mol)	Mg/Ca (mmol/mol)	Mn/Ca (mmol/mol)	Sr/Ca (mmol/mol)
Sandwich Bluff Member—Units 10–14											
Trigoniid bivalve indet.	H5	0.707796	7.2E-06			NA	0.01	0.33	0.35	0.12	2.3
Maorites sp.	H22	0.707829	5.5E-06			4.5	0.01	3.84	2.83	3.09	2.1
Trigoniid bivalve indet.	EV1	0.707758	0.000003			4	0.07	6.63	6.15	11.9	1.29
Eselaevitrigonia sp.	EV2	0.707759	3.6E-06			4.5	0.01	2.28	1.05	0.77	1.81
Eselaevitrigonia sp.	EV3	0.707821	3.6E-06			4	0.01	3.41	2.75	0.14	2
Trigoniid bivalve indet.	EV5	0.707836	4.8E-06			3.5	0.01	1.43	1.67	1.97	3.74
Eselaevitrigonia sp.	EV10	0.707833	0.000005			4	–	–	–	–	–
Eselaevitrigonia sp.	EV11	0.707817	2.6E-06			4	0	0.06	0.3	0.09	1.46
Average		*0.707806*	*0.000021*	*68.5*	*1.45/–1.90*						
Sandwich Bluff Member—Unit 1											
Australoneilo sp.	EV21	0.707807	4.7E-06			3.5	0.04	7.71	5.64	2.63	3.49
– replicate	EV21	0.707794	3.6E-06								
Maorites sp.	EV23	0.707778	3.4E-06			3.5	0.03	7.16	3.16	1.04	3.58
– replicate	EV23	0.707762	4.3E-06								
Bivalve indet.	EV24	0.707775	4.1E-06			NA	0.02	10	5.99	1.39	3.2
– replicate	EV24	0.707792	3.4E-06								
Average		*0.707785*	*0.000012*	*69.7*	*0.45/–1.00*						
U. Cape Lamb Member—270–280 m											
Eutrephoceras sp.	H10	0.707758	4.8E-06			–	–	–	–	–	–
Trigoniid bivalve indet.	EV29	0.707764	5.1E-06			5	0.03	1.65	1.35	0.26	3.34
Average		*0.707761*	*6.4E-06*	*71.0*	*0.15/–0.10*						
L. Cape Lamb Member—234 m											
Trigoniid bivalve indet.	H11	0.707743	8.1E-06			3.5	0.01	0.97	1.41	1.02	2.68
Pinna sp.	EV38	0.707737	7.6E-06			4.5	0.01	4.82	1.07	0.68	4.33
Average		*0.707740*	*6.1E-06*	*71.9*	*0.10/–0.10*						
L. Cape Lamb Member—184 m											
Pinna sp.	EV32	0.707745	4.6E-06			3	0.06	2.25	2.13	1.34	6.65
– replicate	EV32	0.707735	2.8E-06								
Average		*0.707740*	*0.000013*	*71.9*	*0.35/–0.55*						
L. Cape Lamb Member—130–140 m											
Crame et al. (2000)	n = 17	*0.707737*	*1.5E-06*	*72.0*	*0.10/–0.15*	–	–	–	–	–	–
L. Cape Lamb Member—60–130 m											
Eutrephoceras sp.	H14	0.707699	6.8E-06			4	0.16	11.81	1.44	7.07	5.77
Pinna sp.	H15	0.707742	3.2E-06			4	0.07	4.46	2.28	0.7	4.39
Gunnarites sp.	EV15	0.707737	2.6E-06			NA	0.02	1.18	0.99	0.39	3.77
Pyncnodont oyster	EV30	0.707741	3.9E-06			NA	0.01	6.99	5.45	1.24	0.98
– replicate	EV30	0.707725	2.5E-06								
Pinna sp.	EV31	0.707732	3.3E-06			3	0.03	1.11	0.62	0.28	3.74
– replicate	EV31	0.707696	3.9E-06								
Pinna sp.	EV39	0.707696	3.8E-06			3.5	0.03	13.89	9.73	1.5	3.99
Average		*0.707721*	*0.000015*	*72.8*	*0.30/–0.55*						
L. Cape Lamb Member—30–40 m											
Eutrephoceras sp.	H16	0.707749	5.6E-06			4	0.04	0.16	0.55	0.09	5.16
– replicate	H16	0.707719	6.2E-06								
Gunnarites sp.	H17	0.707733	5.7E-06			4	0.05	3	0.69	0.51	4.01
Eutrephoceras sp.	EV25	0.707701	4.1E-06			4	0.03	0.41	0.68	0.24	4.57
Trigoniid bivalve indet.	EV40	0.707712	2.3E-06			3	0.02	3.22	1.03	1.54	1.87
– replicate	EV40	0.707802	3.9E-06								
Pyncnodont oyster	EV41	0.707678	1.15E-05			NA	0.01	0.83	0.4	0.6	0.71
– replicate	EV41	0.707629	8.3E-06								
Gunnarites sp.	EV42b	0.707678	0.000008			NA	–	–	–	–	–
Average		*0.707711*	*0.000029*	*73.1*	*0.60/–1.10*						
Standard—NBS-987	n = 13	0.710233	0.000021								

analyzed. Palynological processing was carried out by one of us (Carey Hannaford) at the MGPalaeo Palynology Laboratory in Malaga, Western Australia. Standard palynological preparatory techniques, as outlined by Phipps and Playford (1984), Wood et al. (1996), and Brown (2008) were used. Additional description of sample processing and images of the specimens are provided in the Supplemental Material.

Samples were analyzed quantitatively using the first 150 recovered specimens in each sample, and any subsequent species were simply recorded as present. Key data and interpretations for each sample are provided in Table 2. Details of the palynomorph assemblages are recorded on the StrataBugs distribution chart, with each taxon expressed as a percentage of the entire assemblage (Supplemental Material Fig. S5; see footnote 1). From this information assignments are made to the Australian palynostratigraphic scheme of MGPalaeo (2014, personal commun.), as shown in Table 2, and based on the schemes of Partridge (2006) and Askin (1988). Finally, the results are also interpreted in terms of the Late Maastrichtian dinoflagellate cyst zonation scheme of Bowman et al. (2012) for Seymour Island.

Magnetostratigraphy

Twenty concretions/concretionary horizons were sampled through the ~100-m-thick Sandwich Bluff Member of the López de Bertodano Formation and the thin, overlying interval of the possible Sobral Formation equivalent (unit SBM16 in this contribution) published by Roberts et al. (2014). Each sample was subdivided into specimens, one of which was measured for paleomagnetism on a 2G Enterprises superconducting quantum interference device (SQUID) magnetometer in the Caltech Paleomagnetics Laboratory using the Rock- and Paleo-magnetic Instrument Development (RAPID) consortium's automatic changer (Kirschvink et al., 2008). For each specimen, natural remanent magnetization was measured, followed by three low-temperature cycling steps in liquid nitrogen, low alternating field demagnetization of up to 7 mT, and then thermal demagnetization of up to 575 °C in 29 steps of 5 °C to 20 °C in a controlled nitrogen atmosphere. Paleomagnetic directions were
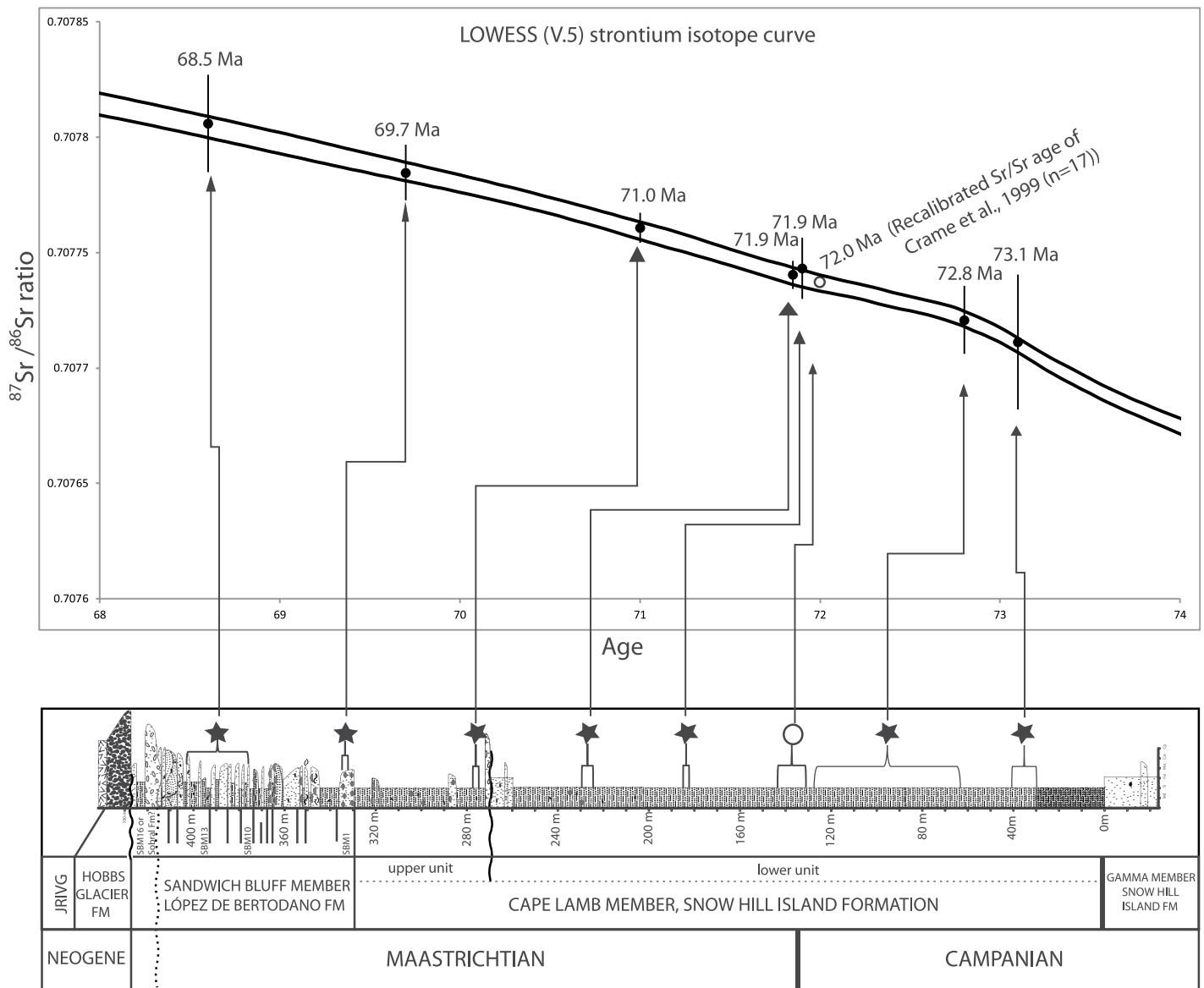
Figure 3. Composite stratigraphic section of Upper Cretaceous succession on Vega Island (bottom), with strontium isotope curve (LOWESS V.5) (top) showing mean $^{87}Sr/^{86}Sr$ results (black dots, 2-sigma error bars) for each of seven binned stratigraphic intervals investigated in this study. Open circle on curve is recalibrated $^{87}Sr/^{86}Sr$ result from Crame et al. (1999). Brackets/stars show stratigraphic location of each sample in section and arrows show where results plot on LOWESS V.5 curve. Upper Cape Lamb Member and Sandwich Bluff Member sections are from Roberts et al. (2014); lower Cape Lamb Member and Gamma Member sections were measured on Cape Lamb in type areas of Pirrie et al. (1991). FM—formation; JRIVG—James Ross Island Volcanic Group.

calculated using the least squares method with anchored lines and planes (Kirschvink, 1980) combined with Fisher statistics (e.g., McFadden and McElhinny, 1990) using the PmagPy software (Tauxe et al., 2016; Figs. 5–6). Beds at Sandwich Bluff were nearly flat-lying with dips of <03° (strike of ~140°); due to the low-degree of post-depositional tilting and the difficulty of determining strike in such a situation, no tilt correction was applied to the data. The measurement level data (with specimen coordinates and stratigraphic position) as well as the interpreted

directions for each specimen with temperature range and maximum angular deviation can be accessed at the MagIC database (for purpose of review: https://earthref.org/MagIC/doi/10.1130 /B6422.1). Additional rock magnetic measurements were performed on selected sister specimens (i.e., taken from the same drill core) of samples representing a range of demagnetization behaviors using a 2G Enterprises SQUID magnetometer following the RAPID protocols and analyzed using the RAPID Matlab scripts (Kirschvink et al., 2008; Fig. S6; see footnote 1).

RESULTS

Sedimentology through Potential K/Pg Interval on Sandwich Bluff

A detailed sedimentological investigation of the top 24 m of the Sandwich Bluff Member (units SBM14–SF2 of Roberts et al., 2014, with SF1-2 herein referred to as SBM16a–SBM16j) was conducted based on fieldwork performed during this study. Rather than a single erosional discontinuity within this interval as originally
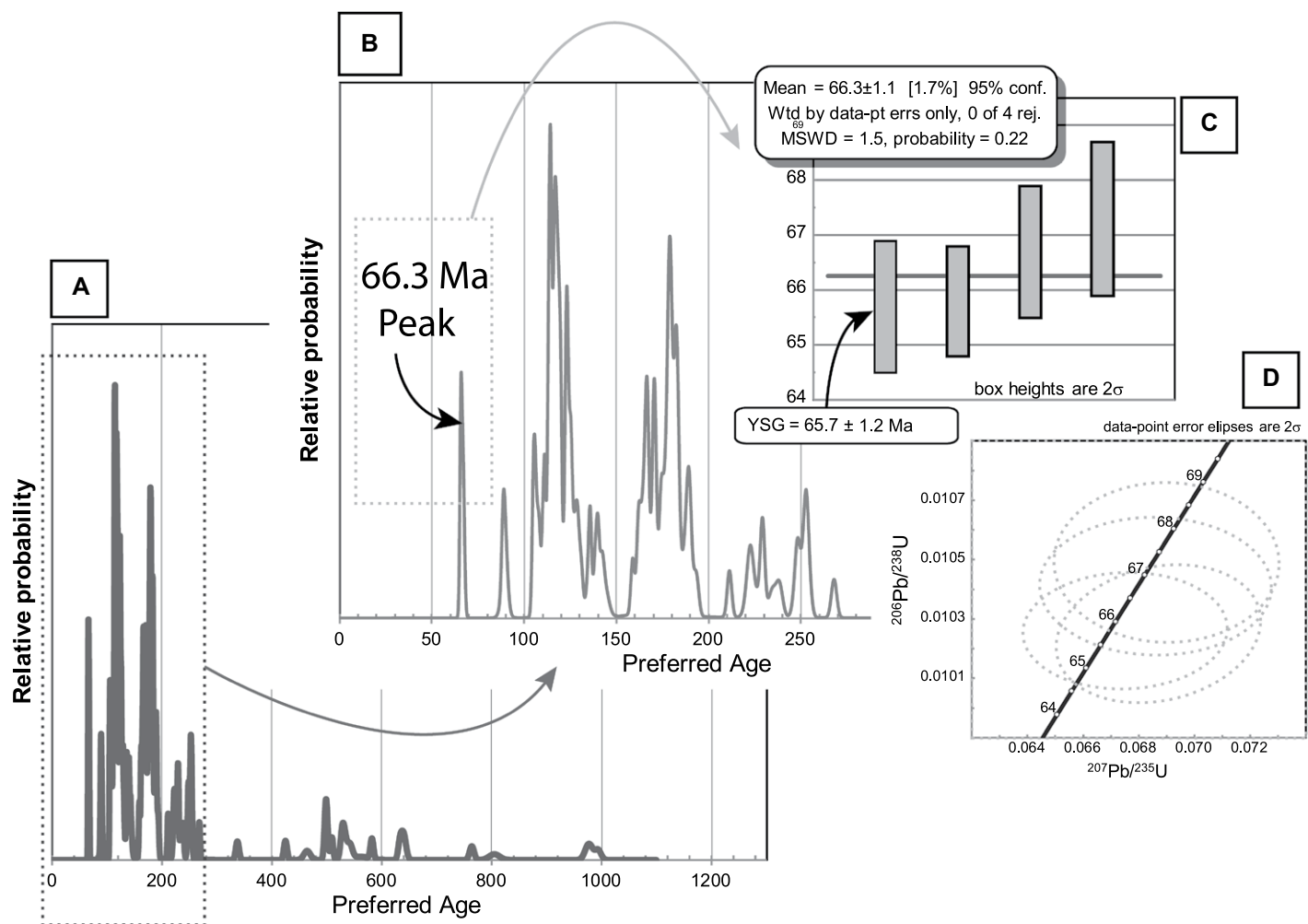
Figure 4. (A) Relative probability plot of detrital zircon sample 22516-9 from unit SBM16j/Sobral Fm? is shown; (B) expanded view of Mesozoic grain ages. Note that the youngest graphical peak age is 66.3 Ma. (C) Weighted mean age of 66.3 ± 1.1 Ma (2σ) for the youngest coherent detrital zircon population composed of four latest Maastrichtian to Paleogene grains. Note the arrow is pointing to the youngest single grain (YSG) at 65.7 ± 1.2 Ma. (D) U-Pb Concordia diagram plots the youngest four grains used to calculate the weighted mean age, which is interpreted to be the maximum depositional age for this horizon.

proposed, there is a series of closely spaced erosional boundaries overlain by upward-fining coarse sandstone to pebble and cobble conglomerates between the base of unit SBM15 and the top of unit SBM16a (this may be Sobral Formation equivalent or unit 10 of the López de Bertodano Formation on Seymour Island; Figs. 2C and 2G). The first of these disconformities is an erosional contact incised into shallow marine sandstones at the top of SBM14, above which a distinctive change in the sedimentology of the section is observed that is characterized by a marked increase in grain size (coarse pebbly sandstone to conglomerate) with abundant intraformational and extraformational pebbles and cobbles. Rounded, intermediate volcanic pebbles and cobbles of up to 35 cm in diameter are most common and are typically matrix-supported within coarse sandstones to granul-

estones (Figs. 2B–2C). This interval has a distinctly alluvial character, and the basal erosional disconformity at the base of SBM15 is herein interpreted to record the initial base-level fall (sequence boundary), which is 2.5 m lower in the section than was originally suggested by Roberts et al. (2014). However, the 3 m interval between the base of units SBM15 and SBM16a is characterized by what appears to be a significant basinward facies shift above a series of disconformities, which suggests a forced regression succeeded by a period of low accommodation and either channel migration/avulsion or minor base-level adjustments.

The section fines upward from here through units SBM16b–SBM16c, which are characterized by abundant plant hash and fragmentary leaf material (including isolated whole leaves) within reddish-orange sandstone to siltstone.

The top of SBM16c is erosionally incised by a distinctive 30-cm-thick, cobble-pebble conglomerate of unit SBM16d, which preserves a number of indeterminate bone fragments. This unit is sharply overlain by a dark gray organic-rich siltstone unit (SBM16e) with alternating dark gray sandstone and siltstone units above (SBM16f–SBM16i). The sedimentology of units SBM16e–SBM16i is very similar and is distinctive for its high abundance but low diversity of trace fossils, dominated by *Thalassinoides*, *Teichichnus*, and *Planolites*. This suite of trace fossils suggests a return to marine conditions and most likely a nearshore tidal environment based on the abundance of *Teichichnus* and *Thalassinoides* and alternating grain size (Gingras et al., 2012; Knaust, 2018). The capping unit SBM16j has a tuffaceous appearance, with a series of clayey intervals that appear to be bentonitic

TABLE 2. PALYNOLOGICAL DATA SUMMARY

Sample no.	Sample level	Microfossil yield	Preservation	Percentage Microplankton Dinoflag.	Spiny ac.	Other	Spore-pollen	Diversity (*1) Microplankton	Spore-pollen	Dinoflagellate zone (Partridge, 2006)	Spore pollen zone (Partridge, 2006)	Askin (1988) Biozones	Environment (*2)	Key datums
3216-2	SBM16j (top)	High	Excellent	6	<1	2	92	2	32	M. druggii, upper	F. longus– T. lillei	Biozones 3-4	Very nearshore marine	T. lillei, T. waipawaense, M. bertodano, M. seelandica
22516-7	SBM16j (base)	Moderate	Excellent	6	<1	5	89	5	25	M. druggii, upper	F. longus	Biozones 3-4	Very nearshore marine	T. lillei, C. ohaiensis, M. seelandica, G. cf evansii, P. golzowense, M. bertodano
170216-1	SBM15	High	Excellent	0	<1	0	100	0	23		F. longus– T. lillei		Non-marine	T. lillei
22516-4	SBM14	High	Excellent	1	0	2	97	2	23	M. druggii, upper	F. longus– T. lillei	Biozone 4	Marginal marine	T. waipawaense, M. bertodano, M. druggii, T. lillei

*1: Diversity

Very high	30 + species
High	20–29 species
Moderate	10–19 species
Low	5–9 species
Very low	1–4 species

*2: Environment

Environment	Dinoflagellate content %	Dinoflagellate diversity	Freshwater algae content %
Shelfal marine	34–66	High	
Nearshore marine	11–33	Moderate	
Very nearshore marine	5–10	Moderate–low	
Marginal marine	<1–4	Low–very low	
Brackish	0, spiny acritarchs only	Extremely low	
Non-marine (undiff.)	0, no spiny acritarchs	Nil	Low <3

(Fig. 2D). A sample of this bed was collected for detrital zircon geochronology and is discussed below. Unit SBM16j is unconformably overlain by the Neogene Hobbs Glacier Formation. We interpret the entire interval between units SBM16d–SBM16j to represent a shallow, likely tidal marine environment associated with a bay or estuary system (Gingras et al., 2012).

The second objective associated with studying the sedimentology of this part of the stratigraphy on Vega Island in greater detail was to search for physical evidence of a K/Pg boundary interval. No obvious evidence of impact ejecta or a proposed post-event mass mortality horizon (e.g., "fish kill horizon" on Seymour Island; Elliot et al., 1994; Witts et al., 2016) was identified. In addition, we found no evidence of a glauconitic interval in the section similar to that observed on Seymour Island, though such a layer would be unlikely given the much shallower water depths estimated for this location. Although there are no obvious physical indications of the boundary, we resampled this interval with the goal of refining the age of the top of the Sandwich Bluff succession, the results of which are presented below.

Sr-Isotope Stratigraphy

Elemental compositional evaluations identified well-preserved shell samples for age analysis in each stratigraphic member. Elemental concentrations in shells are often used to assess samples for alteration following initial macroscopic and/or microscopic examinations (e.g., Brand, 1989; McArthur et al., 1994; Pagani and Arthur, 1998; Cochran et al., 2010); a loss of Sr and an increase in Fe and Mn is expected following diagenetic recrystallization (e.g., Brand and Veizer, 1980; van Geldern et al., 2006). Elemental analysis of our selected samples identified no clear trend in element concentrations or element/Ca ratios with preservation (Table 1; Fig. S1; see footnote 1). We found no indication of an increase in Sr concentrations with decreasing preservation, as found by Cochran et al. (2010) and Knoll et al. (2016), which is thought to be due to the addition of strontianite to the original shell (Fig. S2; see footnote 1). Considering these results, and the careful selection of shell material with a preservation index (PI) of three or greater (good to excellent preservation), the samples analyzed in this study are considered to be mostly unaltered, and hence, viable for use in Sr-isotope stratigraphy.

The lowest stratigraphic interval on Vega Island that was found to have well-preserved fossils was an interval ~30–40 m above the base of the Cape Lamb Member. After diagenetic evaluation, six different samples were chosen for analysis, three of which were analyzed in duplicate.
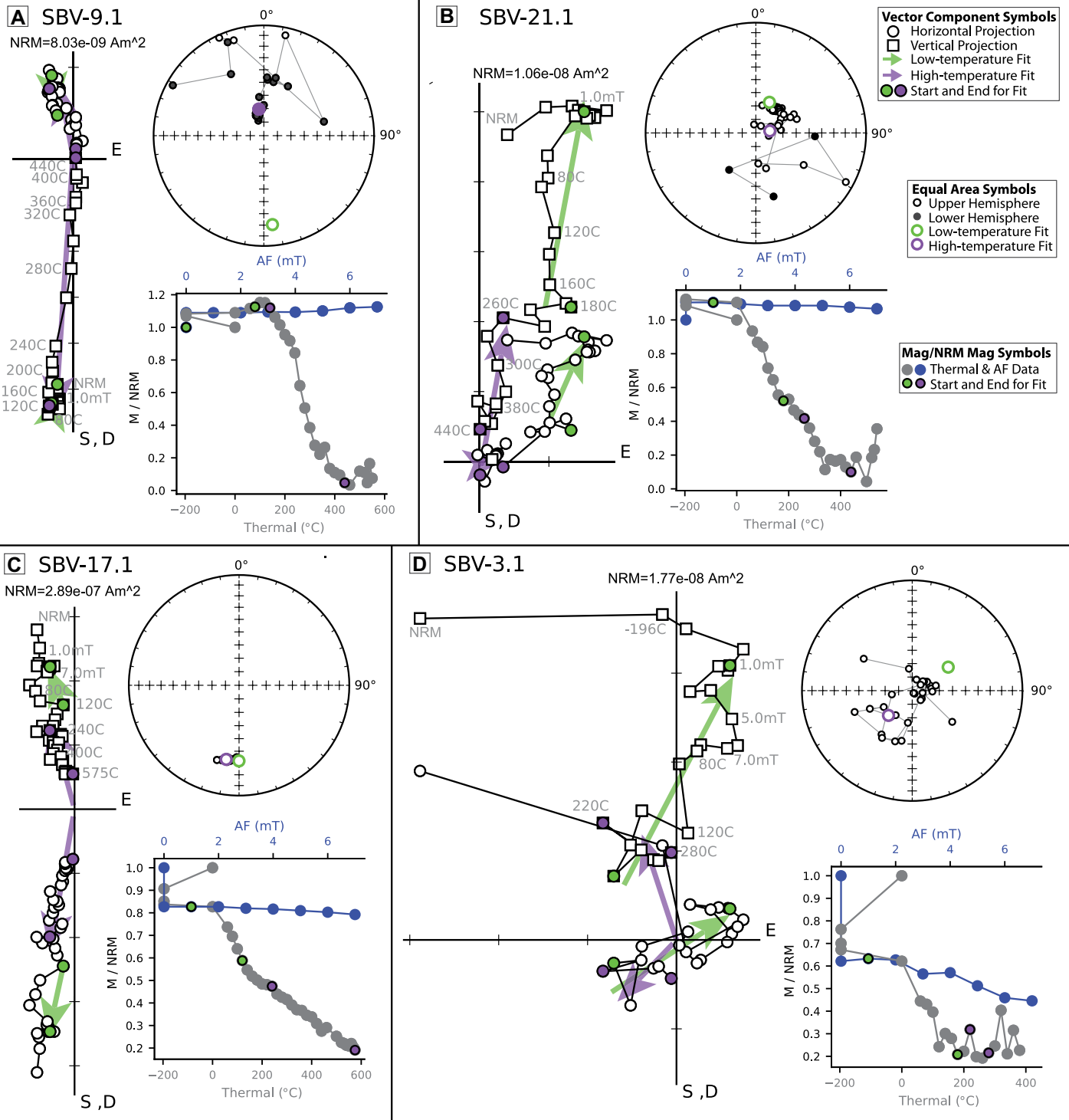
Figure 5. Paleomagnetic data and directional fits are shown. Vector component, equal area, and magnetization/natural remanent magnetization (NRM) plots are shown for four example specimens in in situ coordinates. (A) SBV-9.1 and (B) SBV-21.1 represent two good samples with well-defined, origin-reaching, high-temperature components; the former exemplifies the recorded reversed polarity directions, and the latter displays normal polarity directions that are clearly distinct from a low-temperature component interpreted to be a local field overprint that is present; SBV-21.1 is also the highest sample stratigraphically in this study. (C) SBV-17.1 was one of the three samples that was not fully demagnetized by 575 °C; this sample's rock magnetic properties point to slightly different magnetic mineralogy (Fig. S3; see footnote 1); SBV-17.1 displayed transitional latitudes. (D) SBV-3.1 is an example of a noisy sample that could still be fit with two components, including an origin-trending, high-temperature component. AF—Alternating-Field.
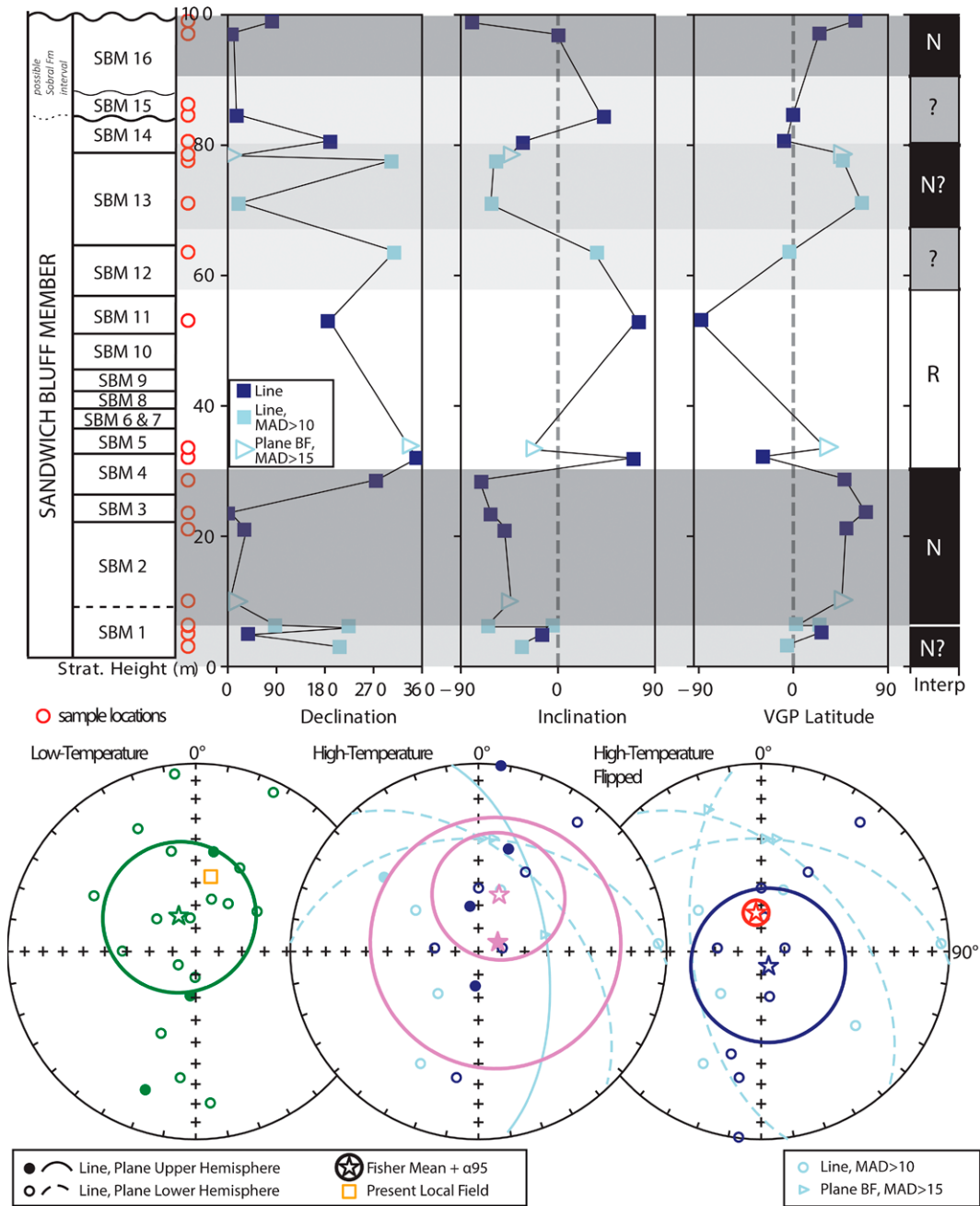
Figure 6. Paleomagnetic results for the Sandwich Bluff Member are presented stratigraphically and in stereographic projection. Polarity interpretations based on virtual geomagnetic pole (VGP) latitude are noted as normal (N) or reverse (R) with sections of uncertain polarity noted with a "?"; high-temperature lines are directional fits using an anchored line, while low-temperature lines are un-anchored. In green on the left-most stereograph, present local field directions of all specimens had a Fisher mean direction (D = 334.5°, I = −72.9°, α95 = 33.3°, N = 20 lines) whose α95 encompasses the present local field when samples were collected (D = 11.4°, I = −56.5°). In purple in the middle stereograph, Fisher means were calculated for normal and reversed polarities, excluding samples in the "?" magnetozones. Normal: D = 20.0°, I = −63.7°, α95 = 28.3°, N = 11 lines, 2 planes; reversed: D = 63.9°, I = 80.7°, α95 = 56.3°, N = 2 lines, 1 plane. In the right stereograph, directions were all flipped to the lower hemisphere to calculate a Fisher mean with robust directions (maximum angular deviation/MAD <10° for lines and <15° for planes): D = 153.0°, I = −83.0°, α95 = 33.8°, N = 10 lines. This mean colored in blue has an α95, which encompasses the mean direction calculated from coeval sediments of Seymour Island (Tobin et al., 2012) colored in red. Plane BF—best fit from plane directional fit.

The mean age for the nine analyses from this interval is 73.1 + 0.6/–1.1 Ma (all errors are reported as 2 s.e.; Table 1; Fig. 3).

Fossil preservation above this level is patchy, and a suite of six well-preserved shells (plus two duplicate analyses) from between 60 and 130 m above the base of the Cape Lamb Member were binned together to determine an age for this interval. The mean age for the eight analyses of this stratigraphic interval is 72.8 + 0.30/–0.55 Ma (Table 1; Fig. 3). Crame et al. (1999)

published a robust Sr-isotope age from the lower Cape Lamb Member based on six shell samples (plus 11 duplicate analyses) from an interval ∼130–145 m above the base of this unit. They calculated a mean age of 71.0 ± 0.2 Ma using Version 2 of the LOWESS curve. Here, we recalibrated this age using the most recent version of the LOWESS curve (Version 5, provided by J. McArthur, 2017, personal commun.) to 72.0 + 0.10/–0.15 Ma (Table 1; Fig. 3, yellow circle). This age is stratigraphically consistent

with ages that we have determined for the intervals below and above this level. In addition, we collected a single, well-preserved bivalve from the interval above this (at 184 m above the base of the Cape Lamb Member) and analyzed it in duplicate. This resulted in a mean age of 71.9 + 0.35/–0.55 Ma (Table 1; Fig. 3), which is also stratigraphically consistent with the recalibrated age of Crame et al. (1999). Two additional shells with excellent preservation were collected from 234 m above the base of the Cape

Lamb Member. These yielded an identical age of 71.9 + 0.10/–0.10 Ma for this interval, which suggests a relatively rapid phase of deposition for the upper portion of the lower Cape Lamb Member and makes it difficult to resolve the age of this interval more precisely.

Only a single interval (between 270 m and 280 m) from the upper unit of the Cape Lamb Member was found to have well-preserved shell material. Two samples were analyzed from this interval, yielding a mean age of 71.0 + 0.15/–0.10 Ma (Table 1; Fig. 3). The lowest unit (SBM1) of the overlying Sandwich Bluff Member of the López de Bertodano Formation preserves comparatively well-preserved shells within the lowest 6 m of the section. Three shells analyzed, each with a duplicate analysis, yielded a mean age of 69.7 + 0.45/–1.0 Ma, which is consistent with existing macrofossil biostratigraphy (Table 1; Fig. 3). Above this, an assortment of very poorly preserved to quite well-preserved shells was collected between 48 m and 82 m (i.e., from units SBM10–SBM13) above the base of this member. Based on the eight shells that passed the PI test from this interval, a mean age of 68.5 + 1.45/–1.90 Ma (2 s.e.) was determined (Table 1; Fig. 3). This age has a relatively higher uncertainty associated with it and is more difficult to reconcile when paired with the micro-biostratigraphy and magnetostratigraphy, both of which suggest a younger age for the sampled interval. Moreover, this part of the stratigraphy rapidly shallows and shows considerable evidence of greater continental influence (e.g., abundant leaves and increasing terrestrial vertebrate fossils). Hence, this stratigraphically highest age within the SBM must be treated with caution.

U-Pb Detrital Zircon Geochronology

The detrital zircon sample analyzed in this study from unit SBM1 (sample 3-5-11-1) at the base of the Sandwich Bluff Member produced 53 concordant analyses out of 56 total analyses. The youngest single zircon grain age was 68.9 ± 0.68 Ma (Table S1; see footnote 1). No other potentially syndepositional latest Cretaceous grains were identified, though, which limits the conclusions that can be drawn from this sample. The MDA provided by this single analysis is consistent with the Sr-isotope results reported above for this stratigraphic interval and with the magnetostratigraphic results discussed below. The majority of the remaining grains yield Early Cretaceous and Jurassic ages, and there was a secondary latest Paleozoic to Neoproterozoic population of grains (see also Pirrie, 1994).

For the highest detrital zircon sample (2-25-16-9), from a tuffaceous interval 2.75 m below the top of the Sandwich Bluff Member or Sobral Formation (unit SBM16j in Fig. 2), a coherent population of four young grains defined by a prominent peak on the frequency distribution curve was documented. This young zircon population yields a robust weighted mean age of 66.3 ± 1.1 Ma for the MDA (Fig. 4; Table S2; see footnote 1), which means that this part of the stratigraphy is latest Maastrichtian in age to earliest Paleogene (Danian). The majority of the other zircon grains in this sample are Early Cretaceous to Triassic in age, and there is a secondary latest Paleozoic–Neoproterozoic population, similar to what was documented in the detrital zircon sample from the base of the Sandwich Bluff Member (Table S2).

Macrofossil Biostratigraphy

Broadly, the few fossils recovered as part of this work do not change previously published interpretations regarding the biostratigraphic relationships of Vega Island with other parts of the James Ross Basin. The Cape Lamb Member of the Snow Hill Island Formation contains abundant examples of the ammonite *Gunnarites*, including those sampled here. *Gunnarites* is part of Ammonite Assemblages 9 and 10 of Olivero (2012) and is found throughout the James Ross Basin and particularly in the eastern half. Invertebrate macrofossils are much less common and are typically poorly preserved in the Sandwich Bluff Member of the López de Bertodano Formation. Early work in this area did not differentiate the Cape Lamb and Sandwich Bluff units, which makes use of their reported occurrences more challenging for biostratigraphy (del Valle and Medina, 1980). Pirrie et al. (1991) reported a non-specific *Maorites* assemblage from the Sandwich Bluff Member, which is consistent with our observations of this unit. Olivero et al. (1992) provided a more detailed faunal analysis but did not sample most or all of what is now the Sandwich Bluff Member.

All ammonite fossils recovered from the Sandwich Bluff Member are most likely *Maorites densicostatus*, which is consistent with all previous findings. The highest *M. densicostatus* specimen recovered was from Sandwich Bluff Member unit SBM14. As in Olivero et al. (1992) and Olivero (2012), we correlate the Sandwich Bluff Member (at least up to unit SBM14) with the upper part (units Klb7–9/10?) of the López de Bertodano Formation on Seymour Island. Though we did not recover any of the formal zonal markers from this interval (e.g., *Pachydiscus* spp.), their absence is likely due to the general paucity and poor preservation of material from the Sandwich Bluff Member. Additionally, based on its occurrence on Seymour Island, *Pachydiscus* likely prefers a deeper water habitat, which making its recovery from the Sandwich Bluff Member unlikely, as it represents an overall shallower marine environment that further shallows significantly from unit SBM14 upwards.

Palynology

The four samples analyzed for palynology each showed excellent preservation and high yields. Paleoenvironmental assessment based on the proportions of marine microplankton (saline algae) to non-marine spores and pollen and freshwater algae, combined with an evaluation of marine microplankton diversity, enable refined environmental subdivision of the top of the Sandwich Bluff Member (Table 2; Fig. 2; Supplemental Material). The results from these four samples confirm a general shallowing-upward succession that transitions from marginal marine (22516-4) to non-marine (170216-1) across the purported sequence-bounding unconformity suggested by Roberts et al. (2014). This is supported by the low percentage (6% or less) and diversity of dinoflagellates, coupled with the very high spore-pollen percentage and diversity in each of the samples. Above this interval, the two highest palynology samples (22516-7 and 3216-2) reveal an increase in dinoflagellate cyst content that is indicative of a return to very near shore to near shore marine conditions (Fig. 2; Table 2; Supplemental Material).

The biostratigraphic assessment of the samples suggests that the entire interval (SBM14–SBM16) likely falls within the Upper Maastrichtian upper subzone of the *Manumiella druggii* dinoflagellate zone within the Australian palynostratigraphic scheme and the *Manumiella druggii* range zone for Antarctica of Bowman et al. (2012). This assignment is indicated by the rare presence of *M. bertodano* with *M. druggi* in sample 22516-4 (SBM14) and the observation of *M. seelandica* in samples 22516-7 and 3216-1. These taxa also indicate zones 3–4 of Askin (1988), whereas the presence of the pollen *Tricolporites lilliei* indicates that the samples fall into the Campanian to Maastrichtian *T. lilliei* to *Forcipites longus* spore pollen zones. In sample 22516-7 (SBM16), the presence of the megaspore *Grapnelispora* cf. *evansii* suggests the *F. longus* spore pollen zone, which provides further support for a latest Maastrichtian age (Table 2; Fig. S5). Samples 22516-7 and 3216-2 were both collected in the thin interval of proposed Paleogene strata (LdB unit 10 or Sobral Formation equivalent strata = unit SBM16j; Fig. 2) at the top of Sandwich Bluff; however, no unequivocally Paleogene restricted dinocysts were encountered in either sample. The extremely low abundances of dinoflagellates (*Manumiella* sp.) noted from

the top of the Sandwich Bluff Member is in stark contrast to the relative abundances documented from the latest Maastrichtian/early Danian López de Bertodano Formation on Seymour Island by Bowman et al. (2012, 2016). This may be due to the rapidly shallowing to emergent nature of the top of the section on Vega Island, which would have been located in a much more proximal portion of the basin. However, reworking of Maastrichtian taxa into Paleogene rocks cannot be ruled out, as an erosional sequence boundary has been hypothesized to explain the distinct sedimentological shift noted at the contact between the top of the Sandwich Bluff Member and the overlying Sobral Formation (or unit 10 of López de Bertodano Formation; Roberts et al., 2014).

Magnetostratigraphy

Based on coercivity spectra, backfield isothermal remanent magnetization measurements, and thermal demagnetization data (Fig. S3; see footnote 1), the primary ferromagnetic mineral in the Sandwich Bluff Member is (titano)magnetite. Additional rock magnetic measurements suggest this is of detrital origin and falls in the size range of single domain to vortex state (Fig. S3). A second component with high coercivity ($H_{cr'} > 200$ mT) is noted and interpreted to be hematite (e.g., Peters and Dekkers, 2003). The presence of hematite is distinct from previous rock magnetic analyses of older rocks from James Ross Basin (e.g., Milanese et al., 2017, 2019; Tobin et al., 2020) but matches a trend toward higher coercivity and two-component coercivity spectra at the top of the López de Bertodano Formation on Seymour Island (Tobin et al., 2012). Magnetostratigraphy connected these upper 200–300 m of the Seymour section to Chron 30N to Chron 29N of the global polarity time scale (GPTS) spanning the K/Pg boundary (Tobin et al., 2012). The presence of the same mineralogical signal in the Sandwich Bluff Member suggests this signal may represent a basin-wide shift in provenance or depositional/diagenetic conditions. Although not explicitly tested in this work, magnetic iron sulfides have not been identified in the James Ross Basin in previous rock magnetic experiments (Milanese et al., 2017, 2019; Tobin et al., 2020).

All of the 20 samples analyzed for magnetostratigraphy contained a low-temperature component that demagnetized by 60–360 °C (Fig. 5). The direction (D = 334.5°, I = −72.9°, $\alpha95 = 33.3°$, N = 20) is interpreted to represent the present local field overprint (Fig. 6). As a viscous remanent magnetization, low thermal demagnetization removes this overprint, although in some cases limestones carrying vortex state magnetite require laboratory demagnetization

in excess of 300 °C (Borradaile, 1999). Above this temperature, coherent directions trending toward the origin were obtained from all but one of the samples; three plane fits were used (Fig. 5). Samples became unstable with irreproducible magnetization and directions at a wide range of temperatures spanning 300 °C to above 575 °C, when measurements were halted as the three remaining stable samples were all trending toward the origin. Samples similarly displayed a range in magnetization strength and errors from directional fits that were not easily correlated to stratigraphic height. Overall, the most reliable samples lost between 65% and 95% of their original remanence before becoming unstable.

High-temperature directions suggest at least two reversals within the stratigraphic sections with predominantly normal directions near the top and bottom with a reversed interval in the middle (Fig. 6). There could be another normal and reversed magnetozone in the upper part of the section (Fig. 6), but due to samples with high error and samples with transitional inclinations (latitudes near zero), this assignment remains provisional/tentative. The lowermost samples, in Sandwich Bluff Member (SBM1), are also noisy, with inclinations/latitudes around 0, but due to one good quality sample we tentatively interpret the area to be a normal magnetozone (with a "?").

Connecting these polarity intervals to the GPTS in the context of this study presents several different plausible options for interpreting the results. The normal polarity interval(s) at the base of the Sandwich Bluff Member must correlate to either C31N or C30N (or both) based on the biostratigraphic and geochronologic constraints presented above. If the normal polarity zone in the lower Sandwich Bluff Member correlates to C31N through C30N (with C30R undetected), an interpretation we consider most likely, then the two clearly defined reversals above this level indicate that the upper part of the member passes through C29R and into C29N (Fig. 7). Alternatively, if the lower part of the stratigraphy correlates solely with C31N, then the reversed interval above would correlate to C30R and the normal polarity zone at the top to C30N. It is also possible that the two poorly defined normal and reversed magnetozones higher in the stratigraphy are authentic reversals, meaning that the base of the section may begin in C31N, with the top extending into C29N (Fig. 7).

DISCUSSION

Chronostratigraphy of the Cape Lamb Member

The Cape Lamb Member of the Snow Hill Island Formation on Vega Island has tradition-

ally been interpreted as latest Campanian to early Maastrichtian in age based on a combination of biostratigraphy and a single reported Sr-isotope age (Fig. 8; Pirrie et al., 1991; Crame et al., 1999; McArthur et al., 2000; Olivero, 2012). Herein, we present a significantly expanded Sr-isotope stratigraphy for the Cape Lamb Member based on samples collected from five intervals through this unit, plus a recalibration of the Sr-isotope age for the middle of the lower unit presented by Crame et al. (1999) and McArthur et al. (2000). The results are stratigraphically consistent with one another and with the recalibrated age from Crame et al. (1999) and confirms a Late Campanian to early Maastrichtian age (Figs. 3 and 8). The 71.0 ± 0.3 Ma Sr-isotope age of Crame et al. (1999) recalibrates to $72.0 + 0.10/ -0.15$ Ma using the updated LOWESS lookup curve (V.5), which is consistent with the original interpretation that this level corresponds roughly to the Campanian–Maastrichtian junction, a boundary that has also since been revised to ca. 72.1 ± 0.2 Ma (e.g., Walker et al., 2018).

With the new Sr-isotope age data presented here, we can also estimate an undecompacted sediment accumulation rate of ~11.4 cm/ka between the lowest (73.1 Ma) and highest (71.0 Ma) Cape Lamb Member binned Sr-isotope results and during a time in which ~240 m of rock accumulated (Fig. S7; see footnote 1). Using this rate, we estimate an additional 0.3 Ma was required to accumulate ~35 m of section below the lowest Cape Lamb Member age locality (i.e., below the 73.1 Ma estimate), which provides an age estimate of 73.4 Ma for the boundary between the Cape Lamb Member and the underlying Gamma Member. However, a significant slowdown in the sediment accumulation rate of ~3.2 cm/ka is recorded for the upper Cape Lamb Member (Fig. S7). The entire ~330-m-thick Cape Lamb Member on Vega Island would have been deposited over a maximum span of ~4.2 m.y., between 73.4 Ma and 69.3 Ma, with an average undecompacted sediment accumulation rate of ~7.9 cm/ka (Fig. S7). This is quite different from recent magnetostratigraphic age models for the same interval within the southeast portion of the James Ross Basin, where undecompacted sediment accumulation rates are six to seven times higher (~50.9 cm/ ka) for nearly the same time interval (Milanese et al., 2020). However, a phenomenon of differential sediment accumulation rates across the basin is certainly possible and likely suggested by the sedimentology, as a period of considerable erosion in the NE part of the basin is indicated by the sequence-bounding unconformity (cobble layer) at the contact between the lower and upper Cape Lamb Members. This effect was likely compounded by later stratigraphic
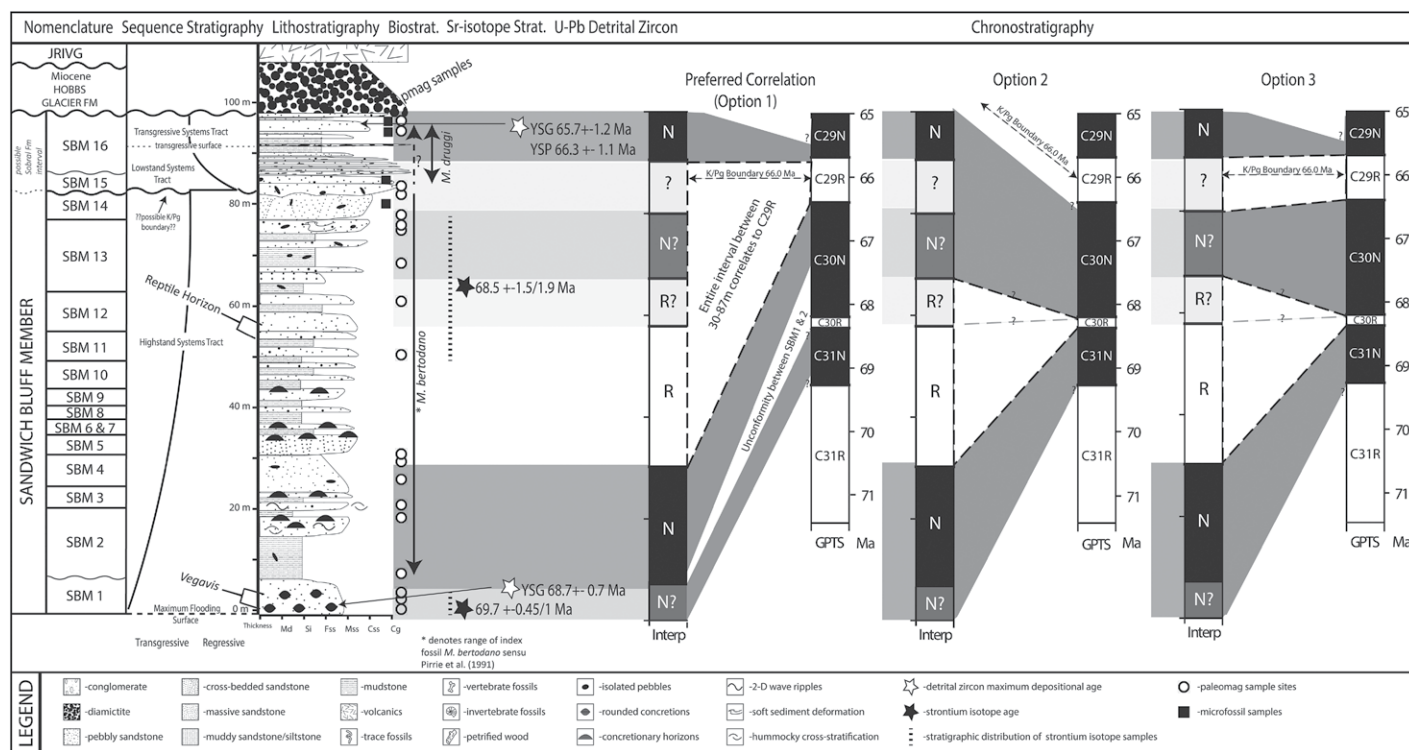
Figure 7. Diagram summarizes the stratigraphy of the Upper Cretaceous (middle–Upper Maastrichtian) Sandwich Bluff Member of the López de Bertodano Formation and overlying units on Vega Island integrating sequence stratigraphy, lithostratigraphy, palynology, Sr-isotope stratigraphy, U-Pb detrital zircon maximum depositional age control, and magnetostratigraphy. Polarity interpretations are noted as normal (N) or reverse (R) with sections of uncertain polarity noted with a "?". Three distinct correlations to the global polarity timescale (GPTS) can be made with the section spanning either: option 1: Chron 31N (C31N) with a hiatus at the top of SBM1, followed by renewed deposition spanning C30N to C29N; option 2: C31N to C30N; or option 3, which includes an interpretation for the sections with uncertain polarity and suggests deposition spanning C31N to C29R. JRIVG—James Ross Island Volcanic Group; SBM—Sandwich Bluff Member. Figure follows the Geomagnetic Polarity Time Scale of Gradstein et al. (2012).

condensation and sediment starvation on the proximal shelf (NW James Ross Basin) during the subsequent maximum transgression at the contact between the Cape Lamb and Sandwich Bluff members, as has been suggested (Olivero, 2012; Roberts et al., 2014). Alternatively, there may be an unconformity and missing time at the contact between the Cape Lamb and Sandwich Bluff Members. This concept was suggested as a possibility by Pirrie et al. (1991); however, both Marenssi et al. (2001) and Olivero (2012) consider this interval to be conformable.

Chronostratigraphy of the Sandwich Bluff Member

Roberts et al. (2014) noted the difficulty of identifying a clear contact between the Cape Lamb and Sandwich Bluff members. They placed the contact of their SBM1, as followed in this study, at the base of a distinctive unit characterized by a rich concentration of carbonate concretions, many of which contain well-preserved fossils and are reminiscent of similar concretion-

ary horizons in the Cape Lamb Member. Based on recent discussions and comparison of the field notes of the authors of this study and previous studies (Pirrie et al., 1991), it appears likely that the beginning of the Sandwich Bluff Member as diagnosed in Pirrie et al. (1991) began above the concretionary level, where the section becomes more recessive at the start of SBM2 of Roberts et al. (2014). This is relevant for discussion of the age of SBM1, which yielded a normal(?) polarity signal, a single young detrital zircon with an age of 68.7 ± 0.7 Ma, and an Sr-isotope age of $69.7 + 0.45/{-}1$ Ma, which suggests that this unit falls within the lower part of C31N.

However, the normal polarity interval above this level (SBM2–SBM4) preserves the first appearance of the temporally diagnostic dinocyst *Manumiella bertodano* (Pirrie et al., 1991; Riding, 1997, unpublished report), which is well-documented to have its first appearance in the upper part of C30N on Seymour Island (broadly between 68 Ma and 67 Ma; Bowman et al., 2014). This strongly suggests that SBM2–SBM4 correlate to C30N and indicates that there

is either an unconformity/hiatus between SBM1 and SBM2 or that the short-duration reversal (C30R) between C31N and C30N was simply not captured/identified due to sampling limitations (see Preferred Correlation in Figs. 7–8). Pirrie et al. (1991) indicated that an unconformity may exist between these two units (i.e., at the top of our SBM1), which supports the former interpretation. Alternatively, it is conceivable that the temporal range of *M. bertodano* on Vega Island extends considerably farther back in time than it does on Seymour Island and that the entire normal polarity interval between SBM1–SBM4 correlates to C31N (see Options 2–3 in Fig. 7). This interpretation is unlikely but remains a possibility.

At the top of SBM4 is a distinct reversed polarity interval that most likely remains reversed polarity (although the samples are ambiguous) until SBM16, where it clearly switches to normal polarity through to the top of the section. Following our preferred interpretation that SBM2–SBM4 correlate to C30N (Option 1; Fig. 7), the distinct reversed polarity
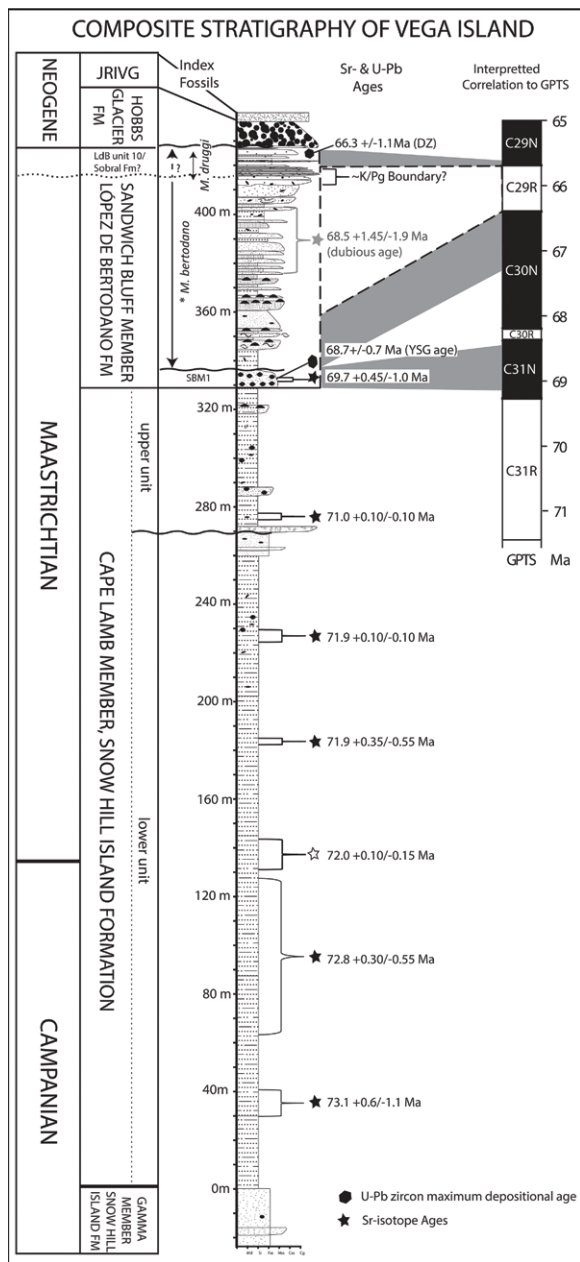
Figure 8. Composite stratigraphic section for Vega Island shows a summary of the updated and legacy biostratigraphy, Sr-isotope stratigraphy, U-Pb age control, interpreted magnetostratigraphy (the preferred correlation in this study), and lithostratigraphy. JRIVG—James Ross Island Volcanic Group; GPTS—Geomagnetic Polarity Time Scale; FM—formation.

based on the identification of both *M. druggi* and *M. seelandica*. However, these samples and those from the 8.4 m below the top of this unit reported by Pirrie et al. (1991) and Riding (1997, unpublished report) also preserve the taxon *M. bertodano*, which was not recovered from the highest samples on Seymour Island. Additionally, no Paleogene taxa were found, except for *M. druggi*, which extends into the early Danian (Bowman et al., 2012). Although the Vega Island succession is much more condensed and proximal to the basin margin, the new samples do suggest that the top of the stratigraphy minimally approaches the K/Pg boundary (66.0 Ma; Walker et al., 2018) as observed on Seymour Island (Bowman et al., 2012). In addition, the palynology supports the sequence stratigraphic interpretation of a transition from marine to non-marine and back to marine conditions at the top of the Sandwich Bluff Member, which potentially correlates with an earliest Paleocene sequence boundary recorded in Seymour Island.

Two alternative interpretations of the stratigraphy are also conceivable; one also supports the presence of a K/Pg boundary, and the other does not. If the normal interval (i.e., SBM1–SBM4) at the base of the section instead correlates exclusively to C31N (Option 2; Fig. 7), it would mean that the reversed polarity interval in the middle of the member (i.e., above SBM4) correlates to C30R and the upper normal polarity interval at the top of Sandwich Bluff correlates to C30N. This interpretation is incongruent with existing interpretations of the age of the base of the *M. bertodano* interval zone. This is also inconsistent with the top of the section that aligns with the *M. druggi* zone. Nonetheless, this interpretation could explain the anomalous (and poor quality) age of the highest Sr-isotope age at 68.5 Ma.

Building on Option 2, another possible correlation exists that includes the paleomagnetic samples in the upper part of the section with high error and samples with transitional inclinations (Fig. 6). If these transitional inclinations represent poorly captured reversals, then the Sandwich Bluff Member passes through five polarity changes, with the base of the section beginning in C31N and the top of the section extending into C29N (shown as Option 3 in Fig. 7). Although this interpretation still suffers from the lack of correspondence between the biostratigraphy (*M. bertodano* interval zone) at the base (similar to option two), it could explain the other data sets (i.e., the Sr-isotope stratigraphy and detrital zircon geochronology) and support the sequence stratigraphic interpretation that a K/Pg boundary is present at the top of the Sandwich Bluff succession.

interval from the top of SBM4 to the base of SBM16 is interpreted to correlate to C29R (consistent with the biostratigraphy on Seymour Island), and the overlying normal polarity interval (upper SBM16) correlates to C29N. This interpretation supports the hypothesis of Roberts et al. (2014) for a K/Pg boundary interval at the top of the Sandwich Bluff Member on Vega Island, an inference previously based on the interpretation of a sequence-bounding unconformity and a return to marine conditions with Sobral Formation-like facies at the top of the section. The single questionable Sr-isotope age from the upper Sandwich Bluff Member (SBM16) recovered in this study is too old to

support this interpretation and is also inconsistent with the biostratigraphy. The mean age of this sample has high uncertainty and is based on a suite of shells collected across a fairly broad and increasingly continentally influenced 30 m interval, and as such, it is considered dubious. The robust detrital zircon MDA of 66.3 ± 1.1 Ma from the top of SBM16, which includes several concordant grains younger than 66 Ma, supports the possibility that the section extends into the early Paleogene. In addition, the new palynological samples from the upper 20 m of the Sandwich Bluff section indicate that the top of the unit passes at least into the very latest Maastrichtian *Manumiella druggi* zone,

Implications for Paleogeography, Paleoenvironments, and Sequence Stratigraphy

The new results presented here also have implications for testing sequence stratigraphic and paleogeographic questions concerning the Sandwich Bluff Member. The more detailed sedimentary logging and palynology presented here for the top 24 m of the stratigraphy on Sandwich Bluff provide crucial support for a sequence boundary and the brief transition to a non-marine depositional system, followed by a rapid return to shallow, possibly estuarine marine conditions (Fig. 2). Roberts et al. (2014) suggested that this putative sequence boundary may correlate to that which caps the Maorites and Grossouvrites (MG) sequence of Olivero (2012) at 66.0 Ma between the top of the López de Bertodano Formation and the base of the Sobral Formation on Seymour Island. In this scenario, the sequence-bounding unconformity would be better developed in the more proximal Vega section than on Seymour Island, which might explain the lack (i.e., erosion) of the post-Cretaceous portion of the López de Bertodano Formation (LdB unit 10) on Sandwich Bluff. Indeed, the conglomeratic interval at this boundary marks a brief period of subaerial exposure and continental deposition ~20 m below the top of the Sandwich Bluff Member and supports the existence of a rapid shallowing event near or after the end of the Cretaceous. This is consistent with observations by Pirrie et al. (1991) for what they believed were rootlets near the top of this member, and it would explain the rapid shallowing event suggested by Macellari (1988) and/or biological change (pre-K/Pg extinction event of primarily benthic invertebrates) recognized near the same interval by Tobin et al. (2012), Tobin (2017), and Mohr et al. (2020) on Seymour Island (however, see Witts et al. (2016) and Whittle et al. (2019) for alternative interpretations). The lack of clear sedimentological evidence recording an earlier (pre-K/Pg) sequence boundary on Seymour Island (*sensu* Tobin, 2017) could be explained by the down-dip relationship between the two localities (see Olivero, 2012; Fig. 2), where the subaerial sequence-bounding unconformity on Vega Island has passed into a correlative conformity in the distal part of the basin on Seymour Island (e.g., Catuneanu et al., 2009). Alternatively, the correlative conformity on Seymour Island may pass through the K/Pg boundary, and the base of Zinsmeister e al.'s (1989) lower Glauconite horizon, which has been described as slightly transgressive, may correlate to the overlying transgressive facies on Vega Island. This may indicate an alternate linkage with the transgressive unit SBM16 and the Paleogene portion

of the López de Bertodano Formation (LdB unit 10) on Seymour Island rather than with the Sobral Formation (e.g., Montes et al., 2019).

Regardless of interpretation, conspicuous differences in the sedimentological character, particularly grain size, of correlative strata of the López de Bertodano Formation on the two islands strongly support existing basin models that indicate the basin depocenter was to the SE and proximal source areas were to the NW (Pirrie et al., 1991; Pirrie, 1994; Hathway, 2000; Olivero, 2012). Sediment supply in the basin most likely outstripped accommodation space, continually shifting the center of deposition to the SE. It is difficult to determine whether the observed sequence boundary and associated landward facies shifts are related to eustatic versus local, tectonically driven sea-level changes; however, the latter is likely given the tectonically active back-arc setting of the James Ross Basin.

Age of *Vegavis* and the Antiquity of the Avian Crown Clade

The holotype and referred specimens of *Vegavis iaai*, recovered from the base of the Sandwich Bluff Member (unit SBM1) on Vega Island, represent the most complete skeletal material of a Mesozoic representative of the avian crown clade (referred to as Anseriformes; Clarke et al., 2005, 2016). Recently, the discovery of an intriguing skull and partial postcranial skeleton of *Asteriornis maastrichtensis* was referred to the avian crown (Field et al., 2020; Torres et al., 2021) from the Late Maastrichtian of Belgium. Field et al. (2020) interpreted *Asteriornis*, dated to 66.8–66.7 Ma, to be some 200 ka older than *Vegavis*, which they regarded as 66.5 Ma in age, citing Ksepka and Clarke (2015). Ksepka and Clarke (2015) actually only advocated 66.5 Ma as the most conservative minimum calibration age. They noted the unit containing the holotype was previously identified as being near the base of the dinoflagellate *M. bertodano* zone (Clarke et al., 2005), and this biozone itself terminated well below the K/Pg boundary (Thorne et al., 2009; Bowman et al., 2012, 2014; reviewed Ksepka and Clarke, 2015), which makes it likely older than *Asteriornis* and the hard minimum bound on calibration given.

Based on refined chronostratigraphy presented herein for the Sandwich Bluff Member, the likely placement of the *Vegavis* horizon (unit SBM1) is ~2–3 m.y. older than the referenced date of *Vegavis* in Field et al. (2020). We interpret the *Vegavis* locality to lie within C31N (Fig. 7), which equates to a numerical age between ca. 69.2 Ma and 68.4 Ma following chron boundary ages in Gradstein et al. (2012). *Vegavis*, based on our best-supported age estimates, is still consid-

ered among the oldest phylogenetically placed representative of the avian crown clade. It is consistent with previous hypotheses of a Gondwanan (=Southern Hemisphere) origin of Aves during the Late Cretaceous (e.g., Claramunt and Cracraft, 2015), but this hypothesis does not explain European finds of approximately the same age (Field et al., 2020). These latest Cretaceous fossils, and better constrained dates on containing units, have the potential to further refine such hypotheses and lead to better evaluation of potential survivorship in the high southern latitudes (Bono et al., 2016; Clarke et al., 2016; Torres et al., 2021).

Age of Non-Avian Dinosaur Localities in the Cape Lamb and Sandwich Bluff Members

In addition to the avifauna from Vega Island, the revised ages reported here also constrain a number of important non-avian dinosaur specimens recovered from the Sandwich Bluff and Cape Lamb members on Vega, James Ross, and Humps Islands. Arguably, the most important interval for preserving diagnostic dinosaur material from the Cape Lamb Member is within the middle portion of this unit (~100–175 m above the base) and includes type localities for *Imperobator antarcticus*, *Morrosaurus antarcticus*, and the "British Antarctic Survey ornithopod" (see Lamanna et al., 2019, for full discussion of the stratigraphy). The Sr-isotope results indicate that these specimens are around 72 Ma in age (Figs. 3 and 8). Refinement of the base of the Cape Lamb Member to roughly 73.4 Ma also places an upper boundary on the age of the Gamma Member of the Snow Hill Island Formation, which indicates that the Santa Marta Cove dinosaur fauna (e.g., the anklylosaur *Antarctopelta oliveroi* and the early-diverging ornithopod *Trinisaura santamartaensis)* is Late Campanian rather than early Maastrichtian. Higher in the stratigraphy, the fossiliferous "reptile horizon" on Sandwich Bluff has produced a suite of important dinosaur fossils that indicates the presence of ankylosaurs, early diverging ornithopods, hadrosaurs, and possibly non-avian theropod dinosaurs. The "reptile horizon," which is characterized by a deflation surface of mostly isolated bones, is spread out between the top of SBM11 and the bottom of SBM12 (see Lamanna et al., 2019). However, more generally, there is a major increase in vertebrate fossil concentration encompassing the interval between units SBM10–SBM12. Following dinocyst biostratigraphy of Bowman et al. (2016), this entire interval falls within the Late Maastrichtian *M. bertodano* zone (zone 3 of Askin, 1988). Also, this interval is best interpreted to fall within the reversed

polarity zone assigned to C29R (see our Preferred Correlation, Figs. 7–8); however, a single paleomagnetic sample from the top of SBM12 yielded a virtual geomagnetic pole close to zero, which makes it difficult to assign this transitional interval to either normal or reversed polarity. A latest Maastrichtian age for this important fauna at no older than 66.3 Ma is strongly supported by the presence of *M. bertodano* throughout the clearly reversed magnetozone (C29R) that spans the top of SBM4 to the middle of SBM11, and presumably all the way through SBM15 (Fig. 7). However, the alternative, less parsimonious correlations to the GPTS (options 2 and 3) that would place the "reptile horizon" at the boundary between C30R and C30N (Fig. 8) cannot be completely ruled out.

CONCLUSIONS

New chronostratigraphic and biostratigraphic results provide an improved characterization of the age of the rocks and fossils preserved on Vega Island in the northwestern portion of the James Ross Basin. All results confirm that the Sandwich Bluff Member is mid- to Late Maastrichtian in age, and there is a strong likelihood that the upper part of the unit extends into the earliest Paleocene. Sedimentologic and micropaleontologic data point to at least one sequence boundary and subsequent transgression at the top of the Sandwich Bluff Member, which likely correlates with either the Sobral unconformity or a cryptic unconformity through the K/Pg boundary, as suggested by Zinsmeister et al. (1989), below the lower Glauconite unit on Seymour Island. Moreover, the age of the reptile horizon at ca. 66.3 Ma indicates that marine reptiles and non-avian dinosaurs persisted in Antarctica until the terminal Cretaceous. Finally, the revised chronostratigraphy in the lower part of the Sandwich Bluff Member provides crucial age constraint (ca. 68.4–69.2 Ma) for fossils assigned to the bird *Vegavis iaai* and informs divergence estimates for the avian crown, rendering *Vegavis* as the most ancient member of the group. As with other recent studies of the basin, our results were likely facilitated by increased melting of the ice cover, which has exposed a greater proportion of the stratigraphy.

REFERENCES CITED

Acosta Hospitaleche, C., Jadwiszczak, P., Clarke, J.A., and Cenizo, M., 2019, The fossil record of birds from the James Ross Basin, West Antarctica: Advances in Polar Science, v. 30, p. 251–273.

Askin, R.A., 1988, Campanian to Paleocene palynological succession of Seymour and adjacent islands, northeastern Antarctic Peninsula, *in* Feldmann, R.M., and Woodburne, M.O., eds., Geology and Paleontology of Seymour Island, Antarctic Peninsula: Geological Society of America Memoir 169, p. 131–153, https://doi.org/10.1130/MEM169-p131.

Bono, R.K., Clarke, J., Tarduno, J.A., and Brinkman, D., 2016, A large ornithurine bird (*Tingmiatornis arctica*) from the Turonian High Arctic: Climatic and evolutionary implications: Scientific Reports, v. 6, p. 1–8, https://doi.org/10.1038/srep38876.

Borradaile, G.J., 1999, Viscous remanent magnetization of high thermal stability in limestone, *in* Tarling, D.H., and Turner, P., eds., Palaeomagnetism and Diagenesis in Sediments: Geological Society, London, Special Publication 151, p. 27–42, https://doi.org/10.1144/GSL.SP.1999.151.01.04.

Bowman, V.C., Francis, J.E., Riding, J.B., Hunter, S.J., and Haywood, A.M., 2012, A latest Cretaceous to earliest Paleogene dinoflagellate cyst zonation from Antarctica, and implications for phytoprovincialism in the high southern latitudes: Review of Palaeobotany and Palynology, v. 171, p. 40–56, https://doi.org/10.1016/j.revpalbo.2011.11.004.

Bowman, V.C., Francis, J.E., and Riding, J.B., 2013, Late Cretaceous winter sea ice in Antarctica?: Geology, v. 41, p. 1227–1230, https://doi.org/10.1130/G34891.1.

Bowman, V.C., Francis, J.E., Askin, R.A., Riding, J.B., and Swindles, G.T., 2014, Latest Cretaceous–earliest Paleogene vegetation and climate change at the high southern latitudes: Palynological evidence from Seymour Island, Antarctic Peninsula: Palaeogeography, Palaeoclimatology, Palaeoecology, v. 408, p. 26–47, https://doi.org/10.1016/j.palaeo.2014.04.018.

Bowman, V., Ineson, J., Riding, J., Crame, J., Francis, J., Condon, D., Whittle, R., and Ferraccioli, F., 2016, The Paleocene of Antarctica: Dinoflagellate cyst biostratigraphy, chronostratigraphy and implications for the palaeo-Pacific margin of Gondwana: Gondwana Research, v. 38, p. 132–148, https://doi.org/10.1016/j.gr.2015.10.018.

Brand, U., 1989, Aragonite-calcite transformation based on Pennsylvanian molluscs: Geological Society of America Bulletin, v. 101, p. 377–390, https://doi.org/10.1130/0016-7606(1989)101<0377:ACTBOP>2.3.CO;2.

Brand, U., and Veizer, J., 1980, Chemical diagenesis of a multicomponent carbonate system; 1, Trace elements: Journal of Sedimentary Research, v. 50, p. 1219–1236.

Brown, C., 2008, Palynological Techniques: Association of Stratigraphic Palynologists Publications Special Publications, 137 p.

Case, J.A., Martin, J.E., Chaney, D.S., Reguero, M., Marenssi, S.A., Santillana, S.M., and Woodburne, M.O., 2000, The first duck-billed dinosaur (Family Hadrosauridae) from Antarctica: Journal of Vertebrate Paleontology, v. 20, p. 612–614, https://doi.org/10.1671/0272-4634(2000)020[0612:TFDBDF]2.0.CO;2.

Catuneanu, O., Abreu, V., Bhattacharya, J.P., Blum, M.D., Dalrymple, R.W., Eriksson, P.G., Fielding, C.R., Fisher, W.L., Galloway, W.E., Gibling, M.R., Giles, K.A., Holbrook, J.M., Jordan, R., Kendall, C.G.St.C., Macurda, B., Martinsen, O.J., Miall, A.D., Neal, J.E., Nummedal, D., Pomar, L., Posamentier, H.W., Pratt, B.R., Sarg, J.F., Shanley, K.W., Steel, R.J., Strasser, A., Tucker, M.E., and Winker, C., 2009, Towards the standardization of sequence stratigraphy: Earth-Science Reviews, v. 92, p. 1–33, https://doi.org/10.1016/j.earscirev.2008.10.003.

Cerda, I.A., Paulina Carabajal, A., Salgado, L., Coria, R.A., Reguero, M.A., Tambussi, C.P., and Moly, J.J., 2012, The first record of a sauropod dinosaur from Antarctica: Naturwissenschaften, v. 99, p. 83–87, https://doi.org/10.1007/s00114-011-0869-x.

Chatterjee, S., 2002, The morphology and systematics of *Polarornis*, a Cretaceous loon (Aves: Gaviidae) from Antarctica, *in* Zhou, Z., and Zhang, F., eds., Proceedings, Symposium of the Society of Avian Paleontology and Evolution, 5th, Beijing, June 2000: Beijing, Science Press, p. 125–155.

Claramunt, S., and Cracraft, J., 2015, A new time tree reveals Earth history's imprint on the evolution of modern birds: Science Advances, v. 1, https://doi.org/10.1126/sciadv.1501005.

Clarke, J.A., Tambussi, C.P., Noriega, J.I., Erickson, G.M., and Ketchum, R.A., 2005, Definitive fossil evidence for the extant avian radiation in the Cretaceous: Nature, v. 433, p. 305–309, https://doi.org/10.1038/nature03150.

Clarke, J.A., Chatterjee, S., Li, Z., Riede, T., Agnolín, F., Goller, F., Isasi, M.P., Martinioni, D.R., Mussel, F.J., and Novas, F.E., 2016, Fossil evidence of the avian vocal organ from the Mesozoic: Nature, v. 538, p. 502–505, https://doi.org/10.1038/nature19852.

Cochran, J.K., Kallenberg, K., Landman, N.H., Harries, P.L., Weinreb, D., Turekian, K.K., Beck, A.J., and Cobban, W.A., 2010, Effect of diagenesis on the Sr, O and C isotope composition of Late Cretaceous mollusks from the Western Interior Seaway of North America: American Journal of Science, v. 310, p. 69–88, https://doi.org/10.2475/02.2010.01.

Cordes-Person, A., Acosta Hospitaleche, C., Case, J., and Martin, J., 2020, An enigmatic bird from the lower Maastrichtian of Vega Island, Antarctica: Cretaceous Research, v. 108, https://doi.org/10.1016/j.cretres.2019.104314.

Coria, R.A., Moly, J.J., Reguero, M., Santillana, S., and Marenssi, S., 2013, A new ornithopod (Dinosauria: Ornithischia) from Antarctica: Cretaceous Research, v. 41, p. 186–193, https://doi.org/10.1016/j.cretres.2012.12.004.

Crame, J.A., 2019, Paleobiological significance of the James Ross Basin 30: Advances in Polar Research, v. 30, p. 186–198.

Crame, J.A., Pirrie, D., Riding, J.B., and Thomson, M.R.A., 1991, Campanian–Maastrichtian (Cretaceous) stratigraphy of the James Ross Island area, Antarctica: Journal of the Geological Society, v. 148, p. 1125–1140, https://doi.org/10.1144/gsjgs.148.6.1125.

Crame, J.A., McArthur, J.M., Pirrie, D., and Riding, J.B., 1999, Strontium isotope correlation of the basal Maastrichtian Stage in Antarctica to the European and US biostratigraphic schemes: Journal of the Geological Society, v. 156, p. 957–964, https://doi.org/10.1144/gsjgs.156.5.0957.

Crame, J.A., Francis, J.E., Cantrill, D.J., and Pirrie, D., 2004, Maastrichtian stratigraphy of Antarctica: Cretaceous Research, v. 25, p. 411–423, https://doi.org/10.1016/j.cretres.2004.02.002.

del Valle, R.A., and Medina, F.A., 1980, Nuevos invertebrados fosiles de Cabo Lamb (Isla Vega) y Cabo Morro (Isla James Ross): Contribuciones científicas del Instituto Antártico Argentino, v. 228, p. 51–67.

del Valle, R.A., Elliot, D.H., and MacDonald, D.I.M., 1992, Sedimentary basins on the east flank of the Antarctic

Peninsula: Proposed nomenclature: Antarctic Science, v. 4, p. 477–478, https://doi.org/10.1017/S0954102092000695.

Dickinson, W.R., and Gehrels, G.E., 2009, Use of U-Pb ages of detrital zircons to infer maximum depositional ages of strata: a test against a Colorado Plateau Mesozoic database: Earth and Planetary Science Letters, v. 288, p. 115–125, https://doi.org/10.1016/j.epsl.2009.09.013.

di Pasquo, M., and Martin, J.E., 2013, Palynoassemblages associated with a theropod dinosaur from the Snow Hill Island Formation (lower Maastrichtian) at the Naze, James Ross Island, Antarctica: Cretaceous Research, v. 45, p. 135–154, https://doi.org/10.1016/j.cretres.2013.07.008.

Elliot, D.H., Askin, R.A., Kyte, F.T., and Zinsmeister, W.J., 1994, Iridium and dinocysts at the Cretaceous–Tertiary boundary on Seymour Island, Antarctica: Implications for the K-T event: Geology, v. 22, p. 675–678, https://doi.org/10.1130/0091-7613(1994)022<0675:IADATC>2.3.CO;2.

Ely, R.C., and Case, J.A., 2019, Phylogeny of a new gigantic paravian (Theropoda; Coelurosauria; Maniraptora) from the Upper Cretaceous of James Ross Island, Antarctica: Cretaceous Research, v. 101, p. 1–16, https://doi.org/10.1016/j.cretres.2019.04.003.

Field, D.J., Benito, J., Chen, A., Jagt, J.W.M., and Ksepka, D.T., 2020, Late Cretaceous neoornithine from Europe illuminates the origins of crown birds: Nature, v. 579, p. 397–401, https://doi.org/10.1038/s41586-020-2096-0.

Foley, E.K., Henderson, R.A., Roberts, E.M., Kemp, A.I.S., Todd, C.N., Knutsen, E.M., Fisher, C., Wainman, C.C., and Spandler, C., 2021, Jurassic arc: Reconstructing the lost world of eastern Australia: Geology, v. 49, p. 1391–1396, https://doi.org/10.1130/G49328.1.

Gingras, M.K., MacEachern, J.A., and Dashtgard, S.E., 2012, The potential of trace fossils as tidal indicators in bays and estuaries: Sedimentary Geology, v. 279, p. 97–106, https://doi.org/10.1016/j.sedgeo.2011.05.007.

Gradstein, F.M., Ogg, J.G., Schmitz, M., and Ogg, G., eds., 2012, The Geologic Time Scale 2012: Amsterdam, Elsevier, 1175 p.

Hall, J.L.O., Newton, R.J., Witts, J.D., Francis, J.E., Hunter, S.J., Jamieson, R.A., Harper, E.M., Crame, J.A., and Haywood, A.M., 2018, High benthic methane flux in low sulfate oceans: Evidence from carbon isotopes in Late Cretaceous Antarctic bivalves: Earth and Planetary Science Letters, v. 497, p. 113–122, https://doi.org/10.1016/j.epsl.2018.06.014.

Hathway, B., 2000, Continental rift to back-arc basin: Jurassic–Cretaceous stratigraphical and structural evolution of the Larsen Basin, Antarctic Peninsula: Journal of the Geological Society, v. 157, p. 417–432, https://doi.org/10.1144/jgs.157.2.417.

Howarth, R.J., and McArthur, J.M., 1997, Statistics for Strontium Isotope Stratigraphy: A Robust LOWESS Fit to the Marine Strontium Isotope Curve for the Period 0 to 206 Ma, with Look-Up Table for the Derivation of Numerical Age: The Journal of Geology, v. 105, p. 441–456, https://doi.org/10.1086/515938.

Kirschvink, J.L., 1980, The least-squares line and plane and the analysis of paleomagnetic data: Geophysical Journal of the Royal Astronomical Society, v. 62, p. 699–718, https://doi.org/10.1111/j.1365-246X.1980.tb02601.x.

Kirschvink, J.L., Kopp, R.E., Raub, T.D., Baumgartner, C., and Holt, J.W., 2008, Rapid, precise, and high-sensitivity acquisition of paleomagnetic and rock-magnetic data: Development of a low-noise automatic sample changing system for superconducting rock magnetometers: Geochemistry, Geophysics, Geosystems, v. 9, 1e18, https://doi.org/10.1029/2007GC001856.

Knaust, D., 2018, The ichnogenus *Teichichnus* Seilacher, 1955, Earth-Science Reviews, v. 177, p. 386–403, https://doi.org/10.1016/j.earscirev.2017.11.023.

Knoll, K., Landman, N.H., Cochran, J.K., Macleod, K.G., and Sessa, J.A., 2016, Microstructural preservation of diagenesis on the carbon and oxygen isotope composition of Late Cretaceous aragonitic mollusks from the Gulf Coastal Plain and the Western Interior Seaway: American Journal of Science, v. 316, p. 591–613, https://doi.org/10.2475/07.2016.01.

Ksepka, D.T., and Clarke, J.A., 2015, Phylogenetic vetted and stratigraphically constrained fossil calibrations for Aves: Palaeontologia Electronica, v. 18, p. 1–25.

Lamanna, M.A., Case, J., Roberts, E.M., Arbour, V., Ely, R., Salisbury, S., Clark, J., Malinzak, D., West, A., and O'Connor, P.M., 2019, Late Cretaceous non-avian dinosaurs from the James Ross Basin, Antarctica: Description of new material, updated synthesis, biostratigraphy, and paleobiology: Advances in Polar Science, v. 30, p. 228–250.

Ludwig, K.R., 2008, User's Manual for Isoplot 3.70. A Geochronological Toolkit for Microsoft Excel: Berkeley Geochronology Center Special Publication 4, 72 p.

Macdonald, D.I.M., Barker, P.F., Garrett, S.W., Ineson, J.R., Pirrie, D., Storey, B.C., Whitham, A.G., Kinghorn, R.R.F., and Marshall, J.E.A., 1988, A preliminary assessment of the hydrocarbon potential of the Larsen Basin, Antarctica: Marine and Petroleum Geology, v. 5, p. 34–53, https://doi.org/10.1016/0264-8172(88)90038-4.

Macellari, C.E., 1988, Stratigraphy, sedimentology, and paleoecology of Upper Cretaceous/Paleocene shelf-deltaic sediments of Seymour Island (Antarctic Peninsula), *in* Feldmann, R.M., and Woodburne, M.O., eds., Geology and Paleontology of Seymour Island, Antarctic Peninsula: Geological Society of America Memoir 169, p. 25–53, https://doi.org/10.1130/MEM169-p25.

Marenssi, S.A., Lirio, J.M., and Santillana, S.N., 1992, The Upper Cretaceous of southern James Ross Island, Antarctica, *in* Rinaldi, C.A., ed., Geología de la Isla James Ross: Buenos Aires, Instituto Antártico Argentino, p. 89–99.

Marenssi, S.A., Salani, F.M., and Santillana, S.N., 2001, Geología de cabo Lamb, Isla Vega, Península Antártica: Contribuciones Científicas del Instituto Antártico Argentino, v. 530, p. 1–43.

McArthur, J.M., and Howarth, R.J., 1998, Strontium isotope stratigraphy: LOWESS version 2. A revised best-fit line to the marine Sr-isotope curve for 0 to 206 Ma, with a revised look-up table for derivation of numerical age, *in* Proceedings, Annual Meeting of the American Association of Petroleum Geologists, Salt Lake City: Tulsa, Oklahoma, American Association of Petroleum Geologists, p. 17–20.

McArthur, J.M., Kennedy, W.J., Chen, M., Thirlwall, M.F., and Gale, A.S., 1994, Strontium isotope stratigraphy for Late Cretaceous time: Direct numerical calibration of the Sr isotope curve based on the US Western Interior: Palaeogeography, Palaeoclimatology, Palaeoecology, v. 108, p. 95–119, https://doi.org/10.1016/0031-0182(94)90024-8.

McArthur, J.M., Thirlwall, M.F., Engkilde, M., Zinsmeister, W.J., and Howarth, R.J., 1998, Strontium isotope profiles across K/T boundary sequences in Denmark and Antarctica: Earth and Planetary Science Letters, v. 160, p. 179–192, https://doi.org/10.1016/S0012-821X(98)00058-2.

McArthur, J.M., Crame, J.A., and Thirlwall, M.F., 2000, Definition of Late Cretaceous stage boundaries in Antarctica using strontium isotope stratigraphy: The Journal of Geology, v. 108, p. 623–640, https://doi.org/10.1086/317952.

McArthur, J.M., Howarth, R.J., and Shields, G.A., 2012, Strontium isotope stratigraphy, *in* Gradstein, F.M., Ogg, J.G., Schmitz, M., and Ogg, G., eds., The Geologic Time Scale 2012: Amsterdam, Elsevier, p. 127–144, https://doi.org/10.1016/B978-0-444-59425-9.00007-X.

McFadden, P.L.L., and McElhinny, M.W.W., 1990, Classification of the reversal test in palaeomagnetism: Geophysical Journal International, v. 103, no. 3, p. 725–729, https://doi.org/10.1111/j.1365-246X.1990.tb05683.x.

Milanese, F.N., Olivero, E.B., Kirschvink, J.L., and Rapalini, A.E., 2017, Magnetostratigraphy of the Rabot Formation, Upper Cretaceous, James Ross Basin, Antarctic Peninsula: Cretaceous Research, v. 72, 172e187, https://doi.org/10.1016/j.cretres.2016.12.016.

Milanese, F.N., Olivero, E.B., Raffi, M.E., Franceschinis, P.R., Gallo, L.C., Skinner, S.M., Mitchell, R.N., Kirschvink, J.L., and Rapalini, A.E., 2019, Mid Campanian–lower Maastrichtian magnetostratigraphy of the James Ross Basin, Antarctica: Chronostratigraphical implications: Basin Research, v. 31, 562e583. https://doi.org/10.1111/bre.12334.

Milanese, F.N., Olivero, E.B., Slotznick, S.P., Tobin, T.S., Raffi, M.E., Skinner, S.M., Kirschvink, J.L., and Rapalini, A.E., 2020, Coniacian–Campanian magnetostratigraphy of the Marambio Group: The Santonian–Campanian boundary in the Antarctic Peninsula and the complete Upper Cretaceous–Lowermost Paleogene chronostratigraphical framework for the James Ross Basin: Palaeogeography, Palaeoclimatology, Palaeoecology, v. 555, https://doi.org/10.1016/j.palaeo.2020.109871.

Mohr, R.C., Tobin, T.S., Petersen, S.V., Dutton, A., and Oliphant, E., 2020, Subannual stable isotope records reveal climate warming and seasonal anoxia associated with two extinction intervals across the Cretaceous–Paleogene boundary on Seymour Island, Antarctica: Geology, v. 48, p. 1131–1136, https://doi.org/10.1130/G47758.1.

Montes, M., Beamud, E., Nozal, F., and Santillana, S., 2019, Late Maastrichtian–Paleocene chronostratigraphy from Seymour Island, James Ross Basin, Antarctic Peninsula: Eustatic controls on sedimentation: Advances in Polar Science, v. 30, p. 303–327.

Olivero, E.B., 2012, Sedimentary cycles, ammonite diversity and palaeoenvironmental changes in the Upper Cretaceous Marambio Group, Antarctica: Cretaceous Research, v. 34, p. 348–366, https://doi.org/10.1016/j.cretres.2011.11.015.

Olivero, E.B., and Medina, F.A., 2000, Patterns of Late Cretaceous ammonite biogeography in southern high latitudes: The Family Kossmaticeratidae in Antarctica: Cretaceous Research, v. 21, p. 269–279, https://doi.org/10.1006/cres.1999.0192.

Olivero, E.B., Scasso, R.A., and Rinaldi, C.A., 1986, Revision of the Marambio Group, James Ross Island, Antarctica: Contribuciones Científicas del Instituto Antártico Argentino, v. 331, p. 1–28.

Olivero, E.B., Martinioni, D.R., and Mussel, F.J., 1992, Upper Cretaceous sedimentology and biostratigraphy of western Cape Lamb (Vega Island, Antarctica). Implications on sedimentary cycles and evolution of the basin, *in* Rinaldi, C.A., ed., Geología de la Isla James Ross: Buenos Aires, Instituto Antártico Argentino, p. 147–166.

Olivero, E.B., Ponce, J.J., and Martinioni, D.R., 2008, Sedimentology and architecture of sharp-based tidal sandstones in the upper Marambio Group, Maastrichtian of Antarctica: Sedimentary Geology, v. 210, p. 11–26, https://doi.org/10.1016/j.sedgeo.2008.07.003.

Pagani, M., and Arthur, M.A., 1998, Stable isotopic studies of Cenomanian–Turonian proximal marine fauna from the US Western Interior Seaway, *in* Dean, W.A., and Arthur, M.A., eds., Concepts in Sedimentology and Paleontology, Volume 6: Tulsa, Oklahoma, SEPM (Society for Sedimentary Geology), p. 201–225.

Partridge, A.D., 2006, Jurassic–Early Cretaceous Spore-Pollen and Dinocyst Zonations for Australia, *in* Monteil, E., ed., Australian Mesozoic and Cenozoic Palynology Zonations—Updated to the 2004 Geologic Time Scale: Geoscience Australia Record, 2006/23.

Paton, C., Hellstrom, J., Paul, B., Woodhead, J., and Hergt, J., 2011, Iolite: freeware for the visualisation and processing of mass spectrometric data: Journal of Analytical Atomic Spectrometry, v. 26, p. 2508–2518, https://doi.org/10.1039/c1ja10172b.

Peters, C., and Dekkers, M.J., 2003, Selected room temperature magnetic parameters as a function of mineralogy, concentration and grain size: Physics and Chemistry of the Earth Parts A/B/C, v. 28, no. 16–19, p. 659–667, https://doi.org/10.1016/S1474-7065(03)00120-7.

Petersen, S.V., Dutton, A., and Lohmann, K.C., 2016, End-Cretaceous extinction in Antarctica linked to both Deccan volcanism and meteorite impact via climate change: Nature Communications, v. 7, https://doi.org/10.1038/ncomms12079.

Phipps, D., and Playford, G., 1984, Laboratory techniques for extraction of palynomorphs from sediments: Papers of the Department of Geology, University of Queensland, v. 11, 23 p.

Pirrie, D., 1989, Shallow marine sedimentation within an active margin basin, James Ross Island, Antarctica: Sedimentary Geology, v. 63, p. 61–82, https://doi.org/10.1016/0037-0738(89)90071-7.

Pirrie, D., 1994, Petrography and provenance of the Marambio Group, Vega Island, Antarctica: Antarctic Science, v. 6, p. 517–527, https://doi.org/10.1017/S0954102094000775.

Pirrie, D., Crame, J.A., and Riding, J.B., 1991, Late Cretaceous stratigraphy and sedimentology of Cape Lamb, Vega Island, Antarctica: Cretaceous Research, v. 12, p. 227–258, https://doi.org/10.1016/0195-6671(91)90036-C.

Pirrie, D., Crame, J.A., Lomas, S.A., and Riding, J.B., 1997, Late Cretaceous stratigraphy of the Admiralty Sound region, James Ross Basin, Antarctica: Cretaceous Research, v. 18, p. 109–137, https://doi.org/10.1006/cres.1996.0052.

Reguero, M.A., and Gasparini, Z., 2006, Late Cretaceous–early Tertiary marine and terrestrial vertebrates from James Ross Basin, Antarctic Peninsula: A review, *in* Rabassa, J., and Borla, M.L., eds., Antarctic Peninsula and Tierra del Fuego: 100 Years of Swedish-Argentine Scientific Cooperation at the End of the World: London, Taylor and Francis, p. 55–76.

Reguero, M., Goin, F., Acosta Hospitaleche, C., Dutra, T., and Marenssi, S., 2013a, Late Cretaceous/Paleogene West Antarctica Terrestrial Biota and its Intercontinental Affinities: Dordrecht, Springer Netherlands, 120 p., https://doi.org/10.1007/978-94-007-5491-1.

Reguero, M.A., Tambussi, C.P., Coria, R.A., and Marenssi, S.A., 2013b, Late Cretaceous dinosaurs from the James Ross Basin, West Antarctica: Geological Society, London, Special Publication 381, no. 1, p. 99–116, https://doi.org/10.1144/SP381.20.

Riding, J.B., 1997, A palynological investigation of the Sandwich Bluff Member (Lopez de Bertodano Formation) from Cape Lamb, Vega Island, Antarctic Peninsula: British Geological Survey Unpublished Technical Report WH/97/79R, 7 p.

Riding, J.B., Keating, J.M., Snape, M.G., Newham, S., and Pirrie, D., 1992, Preliminary Jurassic and Cretaceous dinoflagellate cyst stratigraphy of the James Ross Island Area, Antarctic Peninsula: Newsletters on Stratigraphy, v. 26, p. 19–39, https://doi.org/10.1127/nos/26/1992/19.

Rinaldi, C.A., Massabie, A., Morelli, J., Rosenman, H.L., and del Valle, R., 1978, Geologia de la isla Vicecomodoro Marambio: Contribuciones Cientificas del Instituto Antártico Argentino, v. 217, p. 1–44.

Roberts, E.M., Lamanna, M.C., Clarke, J.C., Meng, J., Gorscak, E., Sertich, J.J.W., O'Connor, P.M., Claeson, K.M., and MacPhee, R.D.E., 2014, Stratigraphy and vertebrate paleoecology of Upper Cretaceous–?lowest Paleogene strata on Vega Island, Antarctica: Palaeogeography, Palaeoclimatology, Palaeoecology, v. 402, p. 55–72, https://doi.org/10.1016/j.palaeo.2014.03.005.

Rozadilla, S., Agnolín, F.L., Novas, F.E., Aranciaga Rolando, A.M., Motta, M.J., Lirio, J.M., and Isasi, M.P., 2016, A new ornithopod (Dinosauria, Ornithischia) from the Upper Cretaceous of Antarctica and its palaeobiogeographical implications: Cretaceous Research, v. 57, p. 311–324, https://doi.org/10.1016/j.cretres.2015.09.009.

Schoepfer, S.D., Tobin, T.S., Witts, J.D., and Newton, R.J., 2017, Intermittent euxinia in the high-latitude James Ross Basin during the latest Cretaceous and earliest Paleocene: Palaeogeography, Palaeoclimatology, Palaeoecology, v. 477, p. 40–54, https://doi.org/10.1016/j.palaeo.2017.04.013.

Smith, S.W., 1992, Microplankton from the Cape Lamb Member, López de Bertodano Formation (Upper Cretaceous), Cape Lamb, Vega Island: Antarctic Science, v. 4, p. 337–353, https://doi.org/10.1017/S095410209200049X.

Tambussi, C.P., and Acosta Hospitaleche, C.I., 2007, Antarctic birds (Neornithes) during the Cretaceous–Eocene times: Revista de la Asociación Geológica Argentina, v. 62, p. 604–617.

Tambussi, C.P., Degrange, F.J., De Mendoza, R.S., Sferco, E., and Santillana, S., 2019, A stem anseriform from the early Palaeocene of Antarctica provides new key evidence in the early evolution of waterfowl: Zoological Journal of the Linnean Society, v. 186, no. 3, p. 673–700, https://doi.org/10.1093/zoolinnean/zly085.

Tauxe, L., Shaar, R., Jonestrask, L., Swanson-Hysell, N.L., Minnett, R., Koppers, A.A.P., Constable, C.G., Jarboe, N., Gaastra, K., and Fairchild, L., 2016, PmagPy: Software package for paleomagnetic data analysis and a bridge to the Magnetics Information Consortium (MagIC) Database: Geochemistry Geophysics Geosystems, v. 17, p. 2450–2463, https://doi.org/10.1002/2016GC006307.

Thorn, V.C., Riding, J.B., and Francis, J.E., 2009, The Late Cretaceous dinoflagellate cyst *Manumiella*—biostratigraphy, systematics and palaeoecological signals in Antarctica: Review of Palaeobotany and Palynology, v. 156, p. 436–448, https://doi.org/10.1016/j.revpalbo.2009.04.009.

Tobin, T.S., 2017, Recognition of a likely two phased extinction at the K-Pg boundary in Antarctica: Scientific Reports, v. 7, https://doi.org/10.1038/s41598-017-16515-x.

Tobin, T.S., Ward, P.D., Steig, E.J., Olivero, E.B., Hilburn, I.A., Mitchell, R.N., Diamond, M.R., Raub, T.D., and Kirschvink, J.L., 2012, Extinction patterns, $\delta^{18}O$ trends, and magnetostratigraphy from a southern high-latitude Cretaceous–Paleogene section: Links with Deccan volcanism: Palaeogeography, Palaeoclimatology, Palaeoecology, v. 350–352, p. 180–188, https://doi.org/10.1016/j.palaeo.2012.06.029.

Tobin, T.S., Roberts, E.M., Slotznick, S.P., Biasi, J.A., Clarke, J.A., O'Connor, P.M., Skinner, S.M., West, A.R., Snyderman, L.S., Kirschvink, J.L., and Lamanna, M.C., 2020, New evidence for a Campanian age for the Cretaceous fossil-bearing strata of Cape Marsh, Robertson Island, Antarctica: Cretaceous Research, v. 108, https://doi.org/10.1016/j.cretres.2019.104313.

Todd, C.N., Roberts, E.M., Spandler, C., Huang, H., Knutsen, E., and Rozefels, A., 2019, Refined age and geological context of two of Australia's most important Jurassic vertebrate taxa (*Rhoetosaurus browneI* and *Siderops kehli*), Queensland: Gondwana Research, v. 76, p. 19–25, https://doi.org/10.1016/j.gr.2019.05.008.

Torres, C.R., Norell, M.A., and Clarke, J.A., 2021, Bird neurocranial and body mass evolution across the end-Cretaceous mass extinction: The avian brain shape left other dinosaurs behind: Science Advances, v. 7, no. 31, https://doi.org/10.1126/sciadv.abg7099.

Tucker, R.T., Roberts, E.M., Hu, Y., Kemp, A.I.S., and Salisbury, S.W., 2013, Detrital zircon age constraints for the Winton Formation, Queensland: Contextualizing Australia's Late Cretaceous dinosaur faunas: Gondwana Research, v. 24, p. 767–779, https://doi.org/10.1016/j.gr.2012.12.009.

Tucker, R.T., Roberts, E.M., Kemp, A.A., and Henderson, B., 2016, Large igneous province or long-lived magmatic arc along the eastern margin of Australia during the Cretaceous? Insights from the sedimentary record: Geological Society of America Bulletin, v. 128, p. 1461–1480, https://doi.org/10.1130/B31337.1.

van Geldern, R., Joachimski, M.M., Day, J., Jansen, U., Alvarez, F., Yolkin, E.A., and Ma, X.P., 2006, Carbon, oxygen and strontium isotope records of Devonian brachiopod shell calcite: Palaeogeography, Palaeoclimatology, Palaeoecology, v. 240, p. 47–67, https://doi.org/10.1016/j.palaeo.2006.03.045.

Walker, J.D., Geissman, J.W., Bowring, S.A., and Babcock, L.E., compilers, 2018, Geologic Time Scale v. 5.0: Geological Society of America, https://doi.org/10.1130/2018.CTS005R3C.

West, A.R., Torres, C.R., Case, J.A., Clarke, J.A., O'Connor, P.M., and Lamanna, M.C., 2019, An avian femur from the Late Cretaceous of Vega Island, Antarctic Peninsula: Removing the record of cursorial landbirds from the Mesozoic of Antarctica: PeerJ, v. 7, https://doi.org/10.7717/peerj.7231.

Whittle, R.J., Witts, J.D., Bowman, V.C., Crame, J.A., Francis, J.E., and Ineson, J., 2019, Nature and timing of biotic recovery in Antarctic benthic marine ecosystems following the Cretaceous–Palaeogene mass extinction: Palaeontology, v. 62, p. 919–934, https://doi.org/10.1111/pala.12434.

Wilckens, O., 1911, Die Anneliden, Bivalven, und Gastropoden der Antarktischen Kreideformationen: Wissenschaftliche Ergebnisse der Schwedischen Südpolar-Expedition, 1901–1903: Stockholm, Lithographisches Institut Des Generalstabs, v. 3, p. 1–132.

Witts, J.D., Bowman, V.C., Wignall, P.B., Alistair Crame, J., Francis, J.E., and Newton, R.J., 2015, Evolution and extinction of Maastrichtian (Late Cretaceous) cephalopods from the López de Bertodano Formation, Seymour Island, Antarctica: Palaeogeography, Palaeoclimatology, Palaeoecology, v. 418, p. 193–212, https://doi.org/10.1016/j.palaeo.2014.11.002.

Witts, J.D., Whittle, R.J., Wignall, P.B., Crame, J.A., Francis, J.E., Newton, R.J., and Bowman, V.C., 2016, Macrofossil evidence for a rapid and severe Cretaceous–Paleogene mass extinction in Antarctica: Nature Communications, v. 7, https://doi.org/10.1038/ncomms11738.

Witts, J.D., Newton, R.J., Mills, B.J.W., Wignall, P.B., Bottrell, S.H., Hall, J.L.O., Francis, J.E., and Alistair Crame, J., 2018, The impact of the Cretaceous–Paleogene (K–Pg) mass extinction event on the global sulfur cycle: Evidence from Seymour Island, Antarctica: Geochimica et Cosmochimica Acta, v. 230, p. 17–45, https://doi.org/10.1016/j.gca.2018.02.037.

Wood, G.D., Gabriel, A.M., and Lawson, J.C., 1996, Palynological techniques–processing and microscopy, *in* Jansonius, J., and McGregor, D.C., eds., Palynology: Principles and Application: American Association of Stratigraphic Palynologists Foundation, v. 1, p. 29–50.

Wood, S.A., and Askin, R.A., 1992, Dinoflagellate cysts from the Marambio Group (Upper Cretaceous) of Humps Island: Antarctic Science, v. 4, p. 327–336, https://doi.org/10.1017/S0954102092000488.

Zinsmeister, W.J., 1979, Biogeographic significance of the late Mesozoic and early Tertiary molluscan faunas of Seymour Island (Antarctic Peninsula) to the final breakup of Gondwanaland, *in* Gray, J., and Boucot, A., eds., Historical Biogeography, Plate Tectonics and the Changing Environment: Proceedings of the 37th Annual Biology Colloquium and Selected Papers: Corvallis, Oregon, Oregon State University Press, p. 349–355.

Zinsmeister, W.J., 1982, Review of the Upper Cretaceous–Lower Tertiary sequence on Seymour Island, Antarctica: Journal of the Geological Society, v. 139, p. 779–785, https://doi.org/10.1144/gsjgs.139.6.0779.

Zinsmeister, W.J., 1998, Discovery of fish mortality horizon at the KT boundary on Seymour Island: Re-evaluation of events at the end of the Cretaceous: Journal of Paleontology, v. 72, p. 556–571, https://doi.org/10.1017/S0022336000024331.

Zinsmeister, W.J., 2001, Late Maastrichtian short-term biotic events on Seymour Island, Antarctic Peninsula: The Journal of Geology, v. 109, p. 213–229, https://doi.org/10.1086/319239.

Zinsmeister, W.J., Feldmann, R.M., Woodburne, M.O., and Elliot, D.H., 1989, Latest Cretaceous/earliest Tertiary transition on Seymour Island, Antarctica: Journal of Paleontology, v. 63, p. 731–738, https://doi.org/10.1017/S0022336000036453.